

ANP-10262(NP)  
Revision 0

## Enhanced Option III Long Term Stability Solution

January 2006

Framatome ANP, Inc.

ANP-10262(NP)  
Revision 0

**Enhanced Option III Long Term Stability Solution**

Prepared: Y. Farawila 27.01.2006  
Y. M. Farawila, Consultant Date

Prepared: D. R. Tinkler 1/27/06  
D. R. Tinkler, Engineer Date  
BWR Safety Analysis

Reviewed: D. R. Todd 27-Jan-06  
D. R. Todd, Engineer Date  
Systems Analysis Methods

Reviewed: D. N. Ziabietsev 1/27/06  
D. N. Ziabietsev, Engineer Date  
Nuclear Technology

Approved: J. S. Holm 1/30/06  
J. S. Holm, Manager Date  
Product Licensing

Approved: D. W. Pruitt 1/28/06  
D. W. Pruitt, Manager Date  
Codes & Methods

**U.S. Nuclear Regulatory Commission  
Report Disclaimer**

**Important Notice Regarding the Contents and Use of This Document**

***Please Read Carefully***

This technical report was derived through research and development programs sponsored by Framatome ANP, Inc. It is being submitted by Framatome ANP, Inc. to the U.S. Nuclear Regulatory Commission as part of a technical contribution to facilitate safety analyses by licensees of the U.S. Nuclear Regulatory Commission which utilize Framatome ANP, Inc. fabricated reload fuel or technical services provided by Framatome ANP, Inc. for light water power reactors and it is true and correct to the best of Framatome ANP, Inc.'s knowledge, information, and belief. The information contained herein may be used by the U.S. Nuclear Regulatory Commission in its review of this report and, under the terms of the respective agreements, by licensees or applicants before the U.S. Nuclear Regulatory Commission which are customers of Framatome ANP, Inc. in their demonstration of compliance with the U.S. Nuclear Regulatory Commission's regulations.

Framatome ANP, Inc.'s warranties and representations concerning the subject matter of this document are those set forth in the agreement between Framatome ANP, Inc. and the Customer pursuant to which this document is issued. Accordingly, except as otherwise expressly provided in such agreement, neither Framatome ANP, Inc. nor any person acting on its behalf:

- a. makes any warranty, or representation, express or implied, with respect to the accuracy, completeness, or usefulness of the information contained in this document, or that the use of any information, apparatus, method, or process disclosed in this document will not infringe privately owned rights;
- or
- b. assumes any liabilities with respect to the use of, or for damages resulting from the use of, any information, apparatus, method, or process disclosed in this document.

**Nature of Changes**

Item	Page	Description and Justification
1.	All	This is a new document.

## Contents

Abstract.....	viii
1.0 Introduction .....	1-1
1.1 Background .....	1-1
1.2 Overview of the Option III Long Term Stability Solution .....	1-2
2.0 Challenges to the Option III Solution .....	2-1
2.1 Elevated DIVOM Curve Slopes.....	2-1
2.2 Option III Applicability under Power Uprate Conditions .....	2-2
2.2.1 Extended Power Uprate (EPU) .....	2-2
2.2.2 Extended Flow Windows (EFW).....	2-3
2.3 Overview of the Enhanced Option III Long Term Stability Solution .....	2-3
3.0 Physical Phenomena.....	3-1
3.1 Effect of Channel Instability on DIVOM Curve.....	3-1
3.1.1 Reactor State Deep Inside the Exclusion Region.....	3-1
3.1.2 Interacting Single Channel and Regional Unstable Modes.....	3-3
3.1.3 Summary of Reduced Order Model Demonstration Results.....	3-4
3.1.4 Summary of RAMONA5-FA Demonstration Results.....	3-5
3.2 Effect of Oscillation Characteristics on the Performance of the Detection Algorithm .....	3-8
3.2.1 Relationship between Amplitude Setpoint and Confirmation Count.....	3-9
3.2.2 Statistical Analysis of the Hot Channel Oscillation Amplitude.....	3-10
3.2.2.1 Effect of the Oscillation Growth Ratio.....	3-10
3.2.2.2 Effect of the Oscillation Period .....	3-12
3.3 [ ] .....	3-13
3.3.1 Two-Pump-Trip Transient .....	3-14
3.3.2 [ ] Reduced Order Model Results .....	3-16
3.3.3 [ ] RAMONA5-FA Results .....	3-17
4.0 Elements of the Enhanced Option III .....	4-1
5.0 Licensing Procedure.....	5-1
5.1 Channel Exclusion Definition .....	5-1
5.2 DIVOM Calculation Procedure .....	5-2
5.3 Pre-Oscillation MCPR.....	5-4
5.4 Amplitude Setpoint Analysis Modification.....	5-5
5.5 Identification of Conservatisms in the Licensing Basis .....	5-5
5.6 Applicable Plant Operating Modes.....	5-7
5.7 Sample Plant Calculations .....	5-8
6.0 References.....	6-1

Appendix A	Results of Interacting Regional and Channel Modes using a Reduced Order Model .....	A-1
Appendix B	Results of Interacting Regional and Channel Modes using RAMONA5-FA.....	B-1
Appendix C	Relationship between Amplitude Setpoint and Period-Based Algorithm Confirmation Count .....	C-1

## Tables

B-1	DIVOM Slopes for Cases with the Hot Channel in the Harmonic Eye .....	B-10
B-2	DIVOM Slopes for Cases with the Hot Channel near the Neutral Line.....	B-11

## Figures

3-1	Regional and Channel Decay Ratios as a Function of Core Power.....	3-2
3-2	DIVOM Slope Ratio versus Hot Channel Decay Ratio for Regional Decay Ratio of 1.2.....	3-5
3-3	Example DIVOM Curve with No Single Channel Instabilities .....	3-6
3-4	DIVOM Curve with Unstable Channel in the Harmonic Eye.....	3-7
3-5	DIVOM Curve with Unstable Channel near the Neutral Line.....	3-7
3-6	Effect of Growth Ratio on HCOM.....	3-11
3-7	Impact of Biasing the Growth Ratio Function on Sampling Probability .....	3-11
3-8	Biased Growth Ratio Probability Functions.....	3-12
3-9	Effect of Period on HCOM.....	3-13
3-10	[ ] Instigation of Oscillations Using the Reduced Order Model.....	3-17
3-11	Power Generated Versus Total Core Flow Using RAMONA5-FA .....	3-19
3-12	Core Power Generated Versus Time Using RAMONA5-FA.....	3-19
3-13	Hot Bundle Power versus Time Using RAMONA5-FA .....	3-20
3-14	Hot Bundle CPR versus Time Using RAMONA5-FA.....	3-20
3-15	Core Inlet Subcooling versus Time Using RAMONA5-FA.....	3-21
3-16	[ ] Oscillation Instigation Using RAMONA5-FA.....	3-21

5-1	Example Channel Exclusion Region.....	5-2
5-2	Definition of the DIVOM Calculation Points for EO-III .....	5-4
5-3	STAIF Predicted versus Measured Channel Decay Ratio all Benchmark Tests .....	5-6
5-4	RAMONA5-FA Predicted versus Measured Channel Decay Ratio for ATRIUM™-10 Tests.....	5-7
A-1	Flux Harmonic Growth Using a Linear Hydraulic Model with Regional Decay Ratio of 1.1.....	A-2
A-2	Flux Harmonic Growth to a Limit Cycle Using a Nonlinear Hydraulic Model Regional Decay Ratio of 1.1.....	A-3
A-3	Neutron Flux Oscillations Using a Linear Hydraulic Model.....	A-3
A-4	Neutron Flux Oscillations Using a Nonlinear Hydraulic Model .....	A-4
A-5	DIVOM Curve with a Hot Channel Decay Ratio of 0.90 .....	A-4
A-6	DIVOM Curve with a Hot Channel Decay Ratio of 0.99 .....	A-5
A-7	DIVOM Points for Stable Channel Cases with Varying Nonlinearity .....	A-5
A-8	DIVOM Curve with a Hot Channel Decay Ratio of 1.04.....	A-6
A-9	DIVOM Curve with a Hot Channel Decay Ratio of 1.06 .....	A-6
A-10	DIVOM Curve with a Hot Channel Decay Ratio of 1.08 .....	A-7
A-11	DIVOM Curve with a Hot Channel Decay Ratio of 1.10 .....	A-7
A-12	DIVOM Curve with a Hot Channel Decay Ratio of 1.12 .....	A-8
A-13	DIVOM Slope Elevation versus Hot Channel Decay Ratio for Regional Decay Ratio of 1.1.....	A-8
A-14	DIVOM Slope Elevation versus Hot Channel Decay Ratio for Regional Decay Ratio of 1.2.....	A-9
A-15	DIVOM Slope Elevation versus Hot Channel Decay Ratio for Regional Decay Ratio of 1.126.....	A-9
B-1	Example DIVOM Curve with No Single Channel Instabilities .....	B-2
B-2	DIVOM Curve with Unstable Channel in the Harmonic Eye, 0.5% Regional, 0.0% Global Perturbation .....	B-3
B-3	DIVOM Curve with Unstable Channel in the Harmonic Eye, 1.0% Regional, 0.0% Global Perturbation .....	B-3
B-4	DIVOM Curve with Unstable Channel in the Harmonic Eye, 2.0% Regional, 0.0% Global Perturbation .....	B-4
B-5	DIVOM Curve with Unstable Channel in the Harmonic Eye, 1.0% Regional, 1.0% Global Perturbation .....	B-4
B-6	DIVOM Curve with Unstable Channel in the Harmonic Eye, 1.0% Regional, -1.0% Global Perturbation .....	B-5

B-7	DIVOM Curve with Unstable Channel in the Harmonic Eye, 1.0% Regional, 2.0% Global Perturbation .....	B-5
B-8	DIVOM Curve with Unstable Channel in the Harmonic Eye, 1.0% Regional, -2.0% Global Perturbation .....	B-6
B-9	DIVOM Curve with Unstable Channel near the Neutral Line, 0.5% Regional, 0.0% Global Perturbation .....	B-7
B-10	DIVOM Curve with Unstable Channel near the Neutral Line, 1.0% Regional, 0.0% Global Perturbation .....	B-7
B-11	DIVOM Curve with Unstable Channel near the Neutral Line, 1.0% Regional, 1.0% Global Perturbation .....	B-8
B-12	DIVOM Curve with Unstable Channel near the Neutral Line, 1.0% Regional, 2.0% Global Perturbation .....	B-8
B-13	DIVOM Curve with Unstable Channel near the Neutral Line, 2.0% Regional, 1.0% Global Perturbation .....	B-9
B-14	DIVOM Curve with Unstable Channel near the Neutral Line, 2.0% Regional, 2.0% Global Perturbation .....	B-9

*This document contains a total of 77 pages.*



## Nomenclature

<u>Acronym</u>	<u>Definition</u>
APRM	Average Power Range Monitor
BSP	Backup Stability Protection
BWR	Boiling Water Reactor
BWROG	BWR Owner's Group
CHDR	Channel Decay Ratio
CPR	Critical Power Ratio
D&S	Detect and Suppress
DIVOM	Delta CPR over Initial Versus Oscillation Magnitude
DR	Decay Ratio
EFW	Expanded Flow Window
EO-III	Enhanced Option III
EOOS	Equipment Out Of Service
EPU	Extended Power Uprate
FANP	Framatome ANP
FFTR	Final Feedwater Temperature Reduction
FHOOS	Feedwater Heater Out Of Service
FOM	Figure of Merit
GDC	General Design Criteria
HCOM	Hot Channel Oscillation Magnitude
IMCPR	Initial Minimum CPR
LPRM	Local Power Range Monitor
LTR	License Topical Report
MCPR	Minimum Critical Power Ratio
MCPROL	Minimum Critical Power Ratio Operating Limit
MELLLA	Maximum Extended Load Line Limit Analysis
OOS	Out of Service
OPRM	Oscillation Power Range Monitor
PBDA	Period Based Detection Algorithm

**Nomenclature** *(continued)*

<u>Acronym</u>	<u>Definition</u>
ROM	Reduced Order Model
SLMCPR	Safety Limit MCPR
SLO	Single Loop Operation
USNRC	U.S. Nuclear Regulatory Commission

**Abstract**

Compliance with General Design Criteria GDC 10 and 12 of 10CFR50 Appendix A precludes operating a Boiling Water Reactor (BWR) under oscillatory conditions. Systems based on the Detect & Suppress (D&S) Long Term Stability Solution Option III have been installed in many BWRs. Such systems issue scram signals upon detecting oscillatory neutron flux signals from Local Power Range Monitors (LPRM) grouped into several Oscillation Power Range Monitor (OPRM) cells. The licensing basis of the existing systems does not address situations leading to highly unstable conditions with multiple interacting instability modes. These conditions are anticipated with flow windows extended beyond the MELLLA domain (e.g. MELLLA+), which are typically associated with power uprate. The Enhanced Option III (EO-III) solution presented here is an evolutionary step relying on the existing methodology and hardware, and introducing measures for addressing the reduced stability associated with extended flow window conditions in general and the higher probability of single channel hydraulic instability excitation in particular. The new elements, introduced as enhancements to the existing Option III solution include the introduction of a calculated exclusion region on the power/flow map. This region is protected by reactor scram and is designed to preclude single channel instabilities. The calculation procedures are modified consistent with the introduction of the channel instability exclusion region.

## **1.0 Introduction**

### **1.1 Background**

Boiling water reactors are known for their propensity to undergo growing power and flow oscillations when operated at power-to-flow ratios that are sufficiently high to excite density wave instabilities. Such unstable states can be reached during startup, like in the Columbia Generating Station instability in 1992, or following an anticipated transient such as a recirculation pump trip which occurred in LaSalle Unit 1 in 1988 and Nine Mile Point Unit 2 in 2004. Operating under such unstable conditions is undesirable as growing power and flow oscillations may eventually reach a level sufficiently high to violate thermal limits and threaten the fuel integrity. The anticipated oscillatory modes in BWRs are:

- a. The global mode: In this mode, the density waves in all fuel channels in the core are in phase and their coupling to the neutron kinetics results in total core power oscillations with individual bundle powers oscillating in phase.
- b. The regional mode: In this mode, the density waves in half the fuel bundles are in phase, and out-of-phase with the bundles in the other half of the core. The coupling of the density waves to the neutron kinetics results in the excitation of the first azimuthal mode where the bundle power in half the core oscillates out-of-phase with the power in the bundles of the other half of the core. The net reactor power remains unchanged when the out-of-phase oscillation magnitude is small, making detection of the oscillation more difficult compared with the global mode as the Average Power Range Monitor (APRM) signals are ineffective. Eventually, at high oscillation magnitudes, nonlinear effects will lead to significant response in the net reactor power, but too late to provide protection for fuel thermal limits. The detection of regional oscillations is also complicated by not knowing a priori the orientation of the neutral line, which marks the vertical plane separating the two core sides oscillating out-of-phase. Detectors lying on or near the neutral line experience virtually no oscillations and cannot be used for detection purposes. It is also possible that the neutral line rotates due to the simultaneous excitation of two degenerate subcritical neutron flux harmonics of the azimuthal type. Fortunately, instead of complicating the detection process, the rotating neutral line is helpful as all detectors swept by the rotation of the neutral line are useful in the detection of regional mode instabilities.

- c. Hydraulic instability in individual channels: Density waves can become unstable in a single channel operated under the boundary condition of constant power and pressure drop without reactivity coupling or power feedback. The impact of single channel instabilities on fuel thermal limits is the primary motivation for the Enhanced Option III solution and will be discussed in more detail in Section 3.1.

There are two fundamental approaches to provide protection against reactor oscillations:

- a. Exclusion Zones: Calculations of decay ratios at different operating states in a given cycle are used to define an exclusion zone on the power-flow map where entry is forbidden by manual or automatic means. Buffer zones of increased awareness of instabilities and immediate exit are common for this type of solution. The Long Term Stability Solution Option I-A (Reference 1) belongs to this category.
- b. Detect & Suppress (D&S): In general, the D&S type of solution is based on analysis of the neutron detector signals and initiates a corrective action upon detecting oscillatory behavior indicative of density wave oscillations. The Long Term Stability Solution Option III (Reference 2) is a D&S solution which has been implemented in many BWR plants in the US. An overview is presented here as it is the basis of the current enhanced solution.

## 1.2 ***Overview of the Option III Long Term Stability Solution***

The D&S Option III solution depends on timely detection of oscillatory behavior by applying certain algorithms to the signals of Oscillation Power Range Monitor (OPRM) cells. An OPRM cell signal is a combination signal from a small number of closely-spaced Local Power Range Monitors (LPRMs). The locations of the LPRMs comprising an OPRM cell include detectors from different vertical levels, but must be confined to a relatively small radial region in order for the averaged signal to remain sensitive to the regional mode oscillations, as radially distant monitors with out-of-phase signals will tend to cancel out. The OPRM cell signals are filtered to remove the high frequency noise component, and also filtered to produce an average OPRM cell signal. The filtered signals are thus conditioned for analysis at the frequency band associated with density wave oscillations (approximately  $0.5 \pm 0.2$  Hz).

The OPRM cell signals are analyzed using the Period-Based Detection Algorithm (PBDA), which functions as follows:

- Identify a base period as the time interval between two successive peaks or minima in the signal. The base period must be in a pre-specified range. For example, a frequency band of  $0.5 \pm 0.2$  Hz would correspond to a period range of 1.43 – 3.33 seconds.
- Count subsequent periods which are equal to the base period within a specified period tolerance. The number of successive counts satisfying this condition is the confirmation count. The count is reset to zero when a period is encountered outside the base period range, in which case a new base period will be identified.
- The number of confirmation counts is empirically correlated to the state of stability of the system, where a number of confirmation counts in the range of 11-14 is correlated to unstable behavior, i.e. decay ratio close to or exceeding unity.
- A trip signal initiating an automatic scram is issued when both the confirmation count and the oscillation amplitude exceed their given setpoints.

Any oscillation detection algorithm requires a delay time from the onset of oscillations to reliable recognition. In the case of the period-based detection algorithm used in the Option III application, the time delay is necessitated by the need to reach a threshold confirmation count, where 11-14 counts (6-7 oscillation cycles) are typically required to avoid signal noise causing spurious scrams. The timely suppression of the growing oscillation by scram, while assuring that the Safety Limit Minimum Critical Power Ratio (SLMCPR) is not violated, depends on the following components of the methodology.

- Statistical calculation of the peak oscillation magnitude. This portion of the methodology is plant-specific and captures the effects of the plant specific trip system definition and setpoint on the magnitude of the hot channel oscillation magnitude (HCOM) immediately before its suppression by scram.
- Determination of the minimum critical power ratio (MCPR) margin that exists prior to the onset of the oscillation. This is a cycle-specific calculation that determines the minimum expected MCPR based on specified scenarios, namely a two recirculation pump trip

along the highest rod line and steady state operation at 45% flow and the highest licensed rod line. Recent experience confirms the two-pump-trip to be the limiting scenario.

- The DIVOM curve, which is a calculated relationship between the fractional change in CPR and the hot channel oscillation magnitude.

It should be noted that the main system setpoints, the threshold number of confirmation counts and the amplitude setpoint, are not independent. A minimum number of confirmation counts is required for a given amplitude setpoint. The range of the applicable amplitude setpoints must satisfy the following constraints:

- The minimum amplitude setpoint must be sufficiently large to allow the minimum number of period confirmation counts required for reliable detection of instability and avoidance of spurious scrams due to signal noise, and
- The maximum amplitude setpoint, which is necessary for timely suppression of the oscillation before its amplitude becomes large enough to exceed the thermal limits.

For a given OPRM system configuration, the selection of an OPRM amplitude setpoint determines the HCOM. The HCOM is transformed to a corresponding fractional change in CPR due to the oscillation using the DIVOM curve. Next, the fractional change in CPR is used to assess the margin to the SLMCPR given the initial MCPR. The optimum setpoint should be high enough to allow the PBDA sufficient time for reliable oscillation detection without an undue risk of spurious scrams (i.e. an adequate number of confirmation counts), but must be low enough to preclude the violation of the SLMCPR. The determination of the amplitude setpoint is cycle-specific.

## 2.0 Challenges to the Option III Solution

The Option III LTS solution has been successfully implemented, and considerable industry experience has provided assurance that the solution provides protection against reactor instabilities and that spurious scrams are low probability events.

Challenges to the applicability of the Option III solution as originally licensed and implemented arise from two issues:

- Elevated DIVOM Curve Slopes
- Option III applicability for flow windows outside of the current MELLLA region.

A thorough understanding of these challenges and their resolution through incremental modifications of the Option III solution are the foundation of the Enhanced Option III solution.

### 2.1 *Elevated DIVOM Curve Slopes*

Evaluations by GE identified a non-conservative deficiency in the generic DIVOM curve specified in Reference 3, and GE issued a report to the USNRC under 10 CFR part 21 (d). Specifically, the regional mode DIVOM slopes were found to be significantly higher than the licensed generic curve for conditions of high peak bundle power-to-flow ratios. Similar observations were found for the global mode DIVOM under conditions of high core power-to-flow ratios.

As an interim fix to the problem, GE provided the affected utilities with a Figure of Merit (FOM) correction to the generic DIVOM slope, where the FOM is derived on either a generic or plant-specific basis. The FOM is an empirical concept based on TRACG code experience and is intended to provide conservatism for high power-to-flow cases (functionally dependent on peak bundle power-to-flow ratio for the regional mode and core power-to-flow ratio for the global mode).

The main problem with the increased DIVOM slopes arising from the use of the very conservative FOM correction is that the amplitude setpoint must be lowered to demonstrate protection of the SLMCPR, which increases the potential for the system to trip the plant upon false identification of unstable oscillations.



The BWROG Detect and Suppress Methodology Committee, which re-formed to address the Part 21 challenge, concluded that the best resolution of the potentially non-conservative DIVOM issue was to eliminate the generic DIVOM curve and substitute a cycle-specific DIVOM analysis in the approved Option III framework (See Reference 5).

Framatome ANP\* (FANP) identified the physical cause of the elevated DIVOM curve slopes as interference of the reactivity-coupled regional mode oscillations and hydraulic instabilities in individual channels (Reference 4). The high power-to-flow ratio causes one or more channels to become unstable and decoupled from the rest of the hydraulic channels, and the flow oscillations in such channels can be driven to even higher amplitudes by the oscillating power. The resulting CPR response in the hydraulically unstable channels becomes higher compared with the case with all hydraulically stable channels, thus causing the symptom of elevated DIVOM slopes. It should be emphasized, however, that the increase in calculated DIVOM slopes is not simply a quantitative response to the changed operating conditions, rather a breakdown of the cause and effect relationship between the detected power oscillation and the CPR response. The DIVOM curve becomes undefined under the condition of decoupled hydraulic instability in one or more channels. The new FANP methodology of calculating the DIVOM curve relies on establishing a region protected by a reactor scram, outside of which the existence of such uncoupled hydraulic instabilities are excluded in order to produce a robust (i.e. the DIVOM curve is linear, bounded and is not sensitive to initial perturbations) DIVOM relationship on a cycle-specific basis.

## **2.2 *Option III Applicability under Power Uprate Conditions***

### **2.2.1 Extended Power Uprate (EPU)**

Plants operating at EPU can increase the power levels beyond the original licensed power by increasing the flow rate along the originally licensed control rod line. In that manner, a two pump trip will eventually take the operating state to a power at natural circulation which is similar for the pre-uprate and post-uprate operating domain. The increased cycle energy is generally achieved by changing the core loading strategy, e.g. by increasing the number of fresh fuel assemblies. Such changes are considered adequately in the Option III licensing as the current

---

\* Framatome ANP, Inc. is an AREVA and Siemens company.

practice requires a cycle-specific DIVOM curve for the calculation of the amplitude setpoint. The current practice of applying Option III is therefore adequate for operating under EPU.

### 2.2.2 Extended Flow Windows (EFW)

Operation at uprated power levels may require an extension of the current MELLLA operating domain to much lower flow rates to maintain operational flexibility (e.g. MELLLA+). This means that an inadvertent two pump trip may occur along a higher rod line taking the operating state eventually to natural circulation at a significantly higher power than the current operating domain. This increased power-to-flow ratio is destabilizing and the applicability of the original Option III methodology (Reference 2) has to be revised.

The challenges to the Option III solution due to operation with an EFW are:

- Higher power-to-flow ratio of the hot channels at or near natural circulation increases the likelihood of destabilizing one or more channels to the point that they decouple from the rest of the hydraulic channels. Should this occur, the DIVOM curve methodology which was developed for core wide and regional oscillations, is no longer robust and the calculated DIVOM curve is not well-defined.
- The neutron reactivity-coupled modes (global and/or regional) will also be destabilized due to the increased power-to-flow ratio and the oscillation growth ratios are expected to be higher in the expanded operating domain.

Other impacts of the EFW include the necessity to review the flow band for which the system is armed. Such a change is merely a quantitative setpoint and does not change the basic solution philosophy or its original licensing basis.

## 2.3 ***Overview of the Enhanced Option III Long Term Stability Solution***

As outlined in the previous sections, the licensing basis of the original Option III methodology does not address situations leading to highly unstable conditions where multiple interacting instability modes, particularly with single channel hydraulic instability excitation, become possible. These conditions are anticipated with flow windows extended beyond the MELLLA domain (e.g. MELLLA+). The Enhanced Option III solution detailed in the following sections is an evolutionary step relying on the existing methodology and hardware, and introducing

measures for addressing reduced stability. The new enhancements to the existing Option III solution are:

1. The introduction of a calculated exclusion region on the power/flow map, protected by reactor scram, to preclude single channel instabilities, and
2. The modification of the DIVOM and setpoint calculation procedures consistent with excluding single channel instabilities.

The physical phenomena associated with the performance of the Detect & Suppress solutions under reduced stability operation are discussed in the following section in order to identify the required enhancements. The elements of the enhanced solution are introduced in detail in the subsequent section.

### 3.0 Physical Phenomena

The Enhanced Option III solution is a direct response to the physical phenomena that exist when the core state is brought deep into the instability zone as defined on the power-flow map. The potential for reaching a highly unstable core state following a two pump trip is anticipated for operation at rod lines above the current MELLLA domain. The physical phenomena which are anticipated include multiple mode instabilities, particularly channel hydraulic instabilities combined with regional mode instability. Also, changes to the oscillation characteristics (growth rate and period) relative to the original analysis basis for Option III solution need to be considered.

#### 3.1 *Effect of Channel Instability on DIVOM Curve*

The D&S Solution Option III was licensed to detect and suppress power oscillations of the global or regional type, but single (or few) hydraulic channel oscillations were not included as these were not considered anticipated transients. The rationale behind excluding single channel oscillations was that the limiting (hot channel) decay ratio is always smaller than the neutron coupled global or regional mode decay ratios. Thus, as the reactor system is destabilized gradually, a global or regional oscillation will develop before a single channel oscillation occurs. This rationale is valid under the conditions considered for licensing the solution, but may not remain valid under the significantly less stable conditions characteristic of the EFW rod lines. Operating at the higher rod lines, the reactor can be brought deep inside the stability exclusion zone following a two pump trip such that several unstable oscillation modes can develop simultaneously including the single channel mode. The effect of such multi-mode excitation and its mitigation are central to the present enhancement of the Option III solution.

##### 3.1.1 Reactor State Deep Inside the Exclusion Region

As mentioned above, the hot channel decay ratio is expected to be smaller than the neutron-coupled global or regional mode decay ratios as the operating state approaches the instability boundary (defined as the contour on the power-flow map which separates stable and unstable states of any possible mode). However, it has been observed that different modes are destabilized at different rates, e.g. with increasing power. Specifically, the rate of destabilizing the single channel hydraulic mode is faster than the neutron-coupled modes. This means that although the channel decay ratio is normally smaller than unity as the reactor operating point crosses the instability boundary, further destabilization results in developing high channel decay

ratios which are greater than unity and may even surpass the decay ratio of the dominant neutron-coupled mode. This situation was not considered in the original licensing of the Option III solution, but must be considered for EFW or similar operating strategies capable of bringing the reactor state deeper inside the instability region. Calculations with the frequency domain code STAIF, Reference 6, demonstrate the faster destabilization of the channel hydraulic mode compared with the neutron-coupled modes. Figure 3-1 depicts the decay ratios of the two limiting modes of oscillation, the hot channel and regional modes, as a function of power at natural circulation flow. At low power, all decay ratios are below unity, and the hot channel decay ratio is smaller than the regional decay ratio. As the power increases, both decay ratios increase until the stability threshold is crossed, while the hot channel remains stable. At higher power, the channel decay ratio increases at a faster rate and reaches a higher value than the neutron-coupled mode.

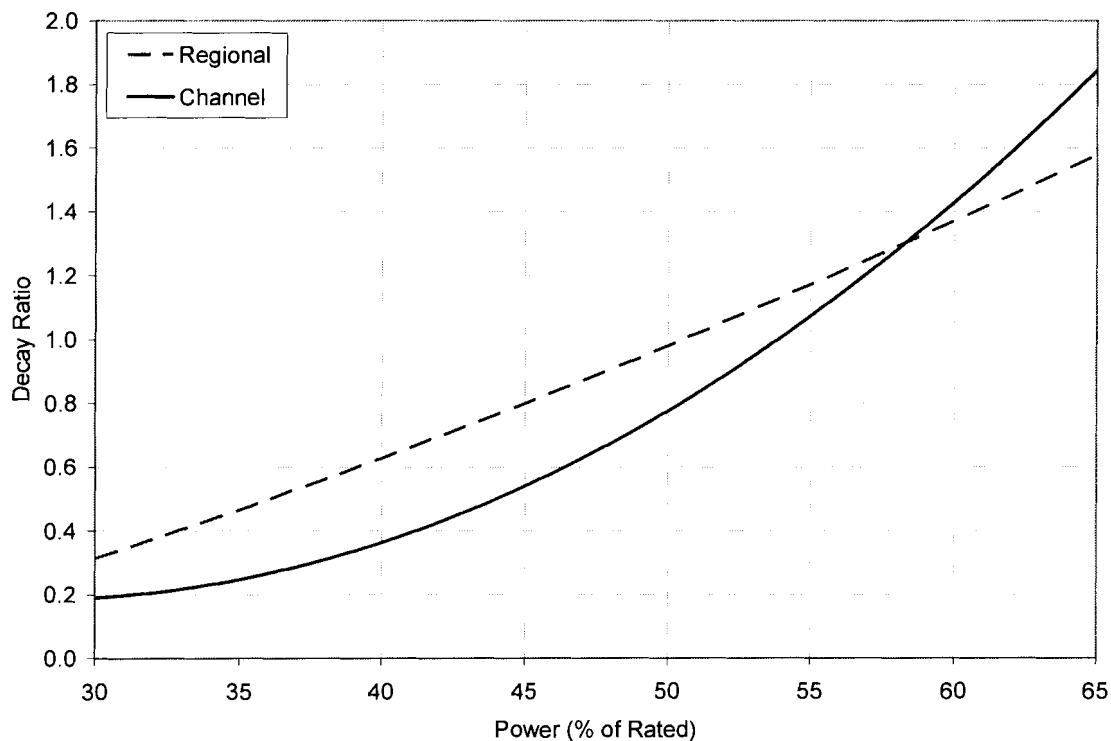


**Figure 3-1 Regional and Channel Decay Ratios as a Function of Core Power**

### 3.1.2 Interacting Single Channel and Regional Unstable Modes

A stable BWR core is a highly coupled system. All the fuel channels are coupled through both hydraulic and neutronic mechanisms.

A single hydraulic channel, considered as a subsystem operated under fixed boundary conditions, can be characterized with its unique damping parameter and resonant frequency. These parameters differ from one channel to another, yet the system of multiple parallel channels is coupled through the common upper and lower plena, and behaves as a coherent system with a common resonant frequency.

The neutronic feedback further augments the coherence of the system. As the neutron kinetics response resulting in coherent power response is spatially distributed according to the fundamental mode or the first azimuthal harmonic, any single channel would be driven by the heating source to conform to the common frequency.

The above picture is qualitatively altered as the system is destabilized. Mathematically, the BWR can be modeled as a dynamic system represented by a set of ordinary nonlinear differential equations where each equation represents the variation of a dynamic variable such as flow or power at a given location. For studying the approach to instability, the dynamic system can be linearized, and a Jacobi matrix constructed. For a stable system, all the complex eigenvalues of the Jacobi matrix have negative real parts. As the system is destabilized, e.g. by gradually increasing power, one eigenvalue acquires a positive real part. This eigenvalue with the positive real part is associated with a neutron-coupled mode such as a global or regional oscillation mode. In this case, all the hydraulic channels continue to act coherently as an in-phase or an out-of-phase oscillation develops. It is highly unlikely that the first eigenvalue to acquire a positive real part corresponds to a single channel hydraulic mode.

The simple picture above is complicated by further destabilization, where not only the magnitude of the real part of the one eigenvalue associated with the single unstable mode increases leading to a faster oscillation growth rate, but more eigenvalues acquire positive real parts. If the second eigenvalue to acquire a positive real part is associated with another neutron-coupled mode to get simultaneous global and regional oscillations, the hydraulic channels continue to behave as a single coherent system responding to a superposition of the

two excited neutron-coupled modes. This situation changes when destabilization continues until an eigenvalue representing a single channel hydraulic mode acquires a positive real part.

The situation of a hydraulic channel mode eigenvalue with a positive real part leads to breaking the coherence of the hydraulic response, and the hot channel starts to respond independently with its own unique resonant frequency. [

]

A further complication of the decoupling of a single channel is that, as the oscillation magnitude increases and nonlinear effects are manifest, the different modes with different resonant frequencies can exchange energy. In this way, the power oscillating at a frequency generally different from that of the single hot channel can boost the channel oscillation magnitude through nonlinear coupling.

As the above phenomena associated with a single hot channel decoupling are quite complicated and hard to quantify, with undesirable consequences such as a DIVOM curve that is no longer robust or even properly defined, the Enhanced Option III solution excludes such phenomena.

The effects of unstable hot channels on the DIVOM curve have been studied using a reduced order model and the full scale system transient code RAMONA5-FA. A summary of these results demonstrating DIVOM departure from regular behavior with unstable hot channels is presented in the next two subsections.

### 3.1.3 Summary of Reduced Order Model Demonstration Results

A multi-channel nonlinear reduced order model (ROM) was fit to realistic reactor parameters for simulating multiple interacting instability modes. While the reactor operating point is regionally

unstable, the hot channel decay ratio, and amount of hydraulic nonlinearity ( $\xi$ ) were varied parametrically to induce its decoupling from the rest of the hydraulic channels and study the effects of its interaction with the neutron-coupled regional mode. The relative effect on the DIVOM curve was obtained from the hot channel hydraulic response as a function of the power oscillation magnitude. The results indicate that the DIVOM curve is no longer robust and its slope significantly increases [

] An example of this behavior is shown in Figure 3-2. More details for this type of analysis are given in Appendix A.



**Figure 3-2 DIVOM Slope Ratio versus Hot Channel Decay Ratio for Regional Decay Ratio of 1.2**

#### 3.1.4 Summary of RAMONA5-FA Demonstration Results

Full-scale calculations using the detailed system code RAMONA5-FA were performed in order to confirm the reduced order model observations regarding the breakdown of DIVOM in the presence of single channel instability interacting with the regional mode oscillations. The two approaches, ROM and detailed system simulations, complement each other in the sense that



deep insights and wide variation of parameters can be achieved with a fast ROM, while few near-exact simulations of actual plant conditions are achieved using system codes. In addition, actual DIVOM curves are calculated by system codes, while only relative variations are available from a reduced order model.

The RAMONA5-FA DIVOM calculations demonstrate that the regular, well-behaved DIVOM curve shown in Figure 3-3, which is typical for licensing analysis, is no longer maintained when channel hydraulic instabilities are present. Examples of ill-defined DIVOM curves with elevated slopes were obtained with an unstable hot channel located in the eye of the azimuthal harmonic (peak of the power oscillation), and located along the neutral line (no significant power oscillation) and are shown in Figure 3-4 and Figure 3-5, respectively. More details of these calculations are presented in Appendix B.

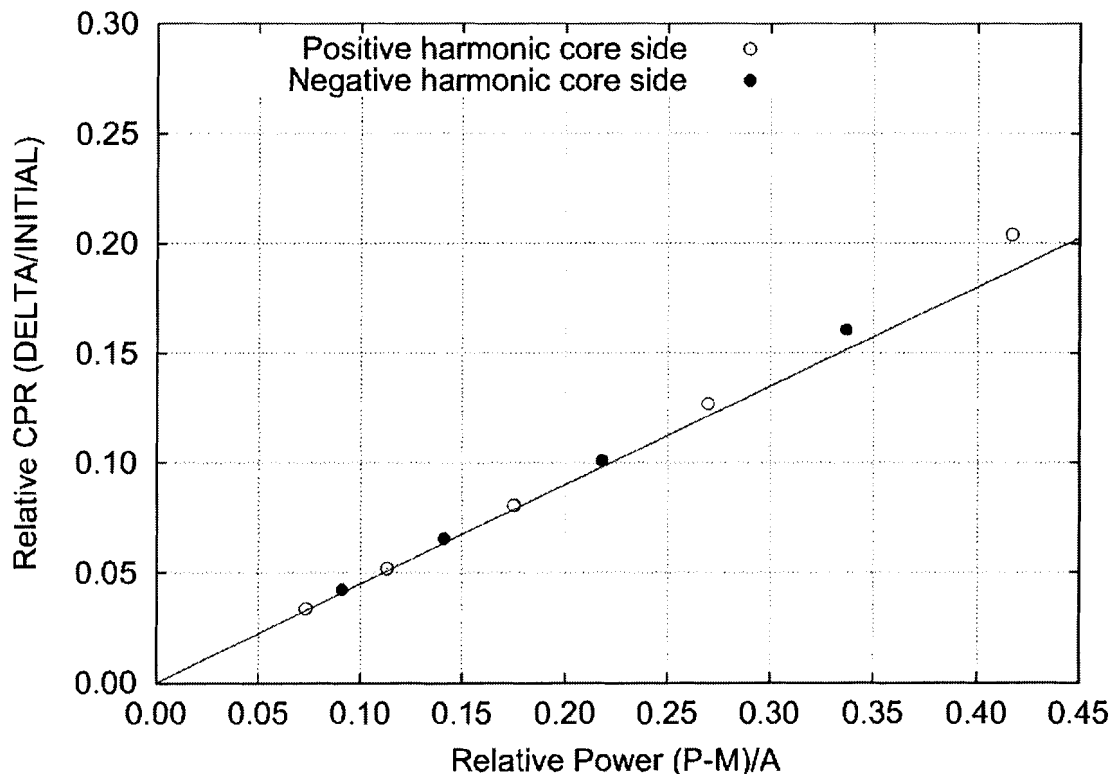


**Figure 3-3 Example DIVOM Curve with No Single Channel Instabilities**

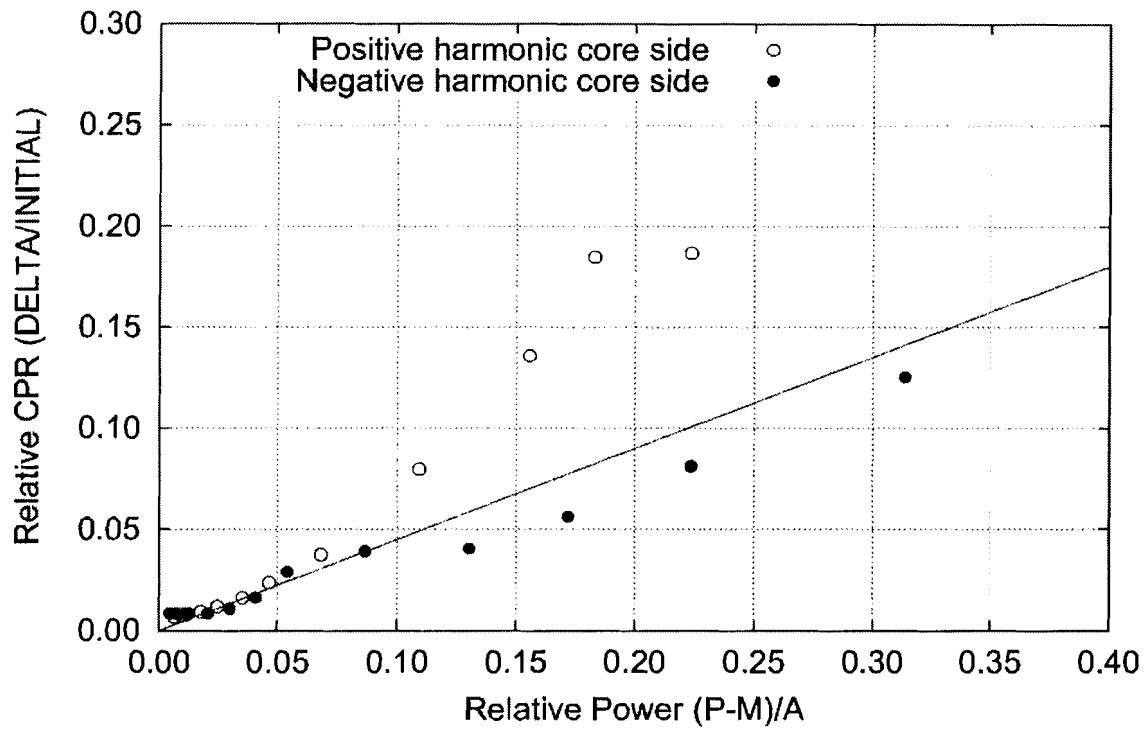


**Figure 3-4 DIVOM Curve with Unstable Channel in the Harmonic Eye**

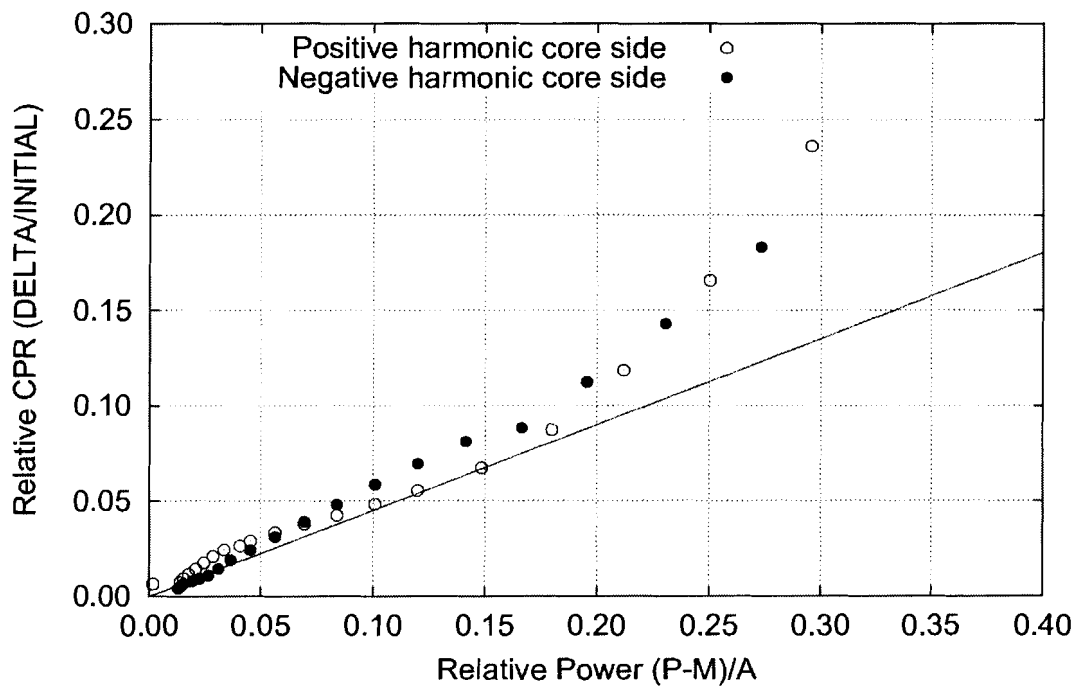


**Figure 3-5 DIVOM Curve with Unstable Channel near the Neutral Line**

### 3.2 ***Effect of Oscillation Characteristics on the Performance of the Detection Algorithm***

The interaction of the Detect & Suppress algorithm with the power signals deserves special attention in order to examine the effects of the altered oscillation characteristics as anticipated from destabilizing operational modes. More specifically, the oscillation growth ratio (and to a lesser extent the oscillation period) may become sufficiently different from their distributions used in the licensing of the original D&S solution, Reference 2.

The effect of the oscillation characteristics on the D&S algorithm can be divided into two distinct segments. The first segment covers the time interval during which the period-based algorithm detects oscillatory behavior and terminates when the signal amplitude crosses the amplitude setpoint. The second segment starts from the end of the first segment, and terminates with the suppression of the oscillation by scram.

Regarding the effect of oscillation growth ratio in the first segment, it is important to note that the PBDA requires a minimum number of confirmation counts (counting peaks and minima at regular time intervals or period) to positively identify oscillating behavior. At the same time, the algorithm is able to detect such peaks only when the effect of noise is not large. Therefore, the magnitude of the useful signal must be above the noise level, which is typically 3% peak-to-peak. The upper limit of the signal amplitude is set by the amplitude and confirmation count setpoints. A growing oscillation therefore must not grow so fast as to not allow enough cycles for the detection algorithm to reach its confirmation counts before the signal reaches the amplitude setpoint. This puts an upper limit, for a given amplitude setpoint, to the growth ratio of a signal that can be detected and suppressed successfully. Equivalently, a higher amplitude setpoint would be required for a given number of confirmation counts in order to cover increased growth ratio.

The potential requirement of increased amplitude setpoint to allow the PBDA sufficient counts for the proper detection of high growth ratio signals competes with the requirement of reasonably low amplitude setpoint in order to allow sufficient time for oscillation suppression prior to violating thermal limits. This concern leads to an examination of the performance of the algorithm in the second segment as well.

It will be shown below that the changes in the oscillation characteristics, growth ratio and period, anticipated from less stable operating modes such as exist in an expanded flow window, do not significantly alter the licensing basis of the original D&S solution.

### 3.2.1 Relationship between Amplitude Setpoint and Confirmation Count

As mentioned in Appendix E of Reference 2, the amplitude setpoint and the number of confirmation counts are not independent. The relationship between these two system setpoints is modeled theoretically for an idealized signal with constant growth ratio and constant oscillation period. This assumption is extremely conservative, and does not allow sufficient confirmation counts should the anticipated growth ratio increase.

More specifically, a growth ratio of 1.3 is specified in Appendix E, Reference 2, which allows 12 confirmation counts for a typical amplitude setpoint of 1.1 (Table E-1 of Reference 2 provides a complete set of confirmation counts versus amplitude setpoint). Under these assumptions, an increased growth ratio by 0.1 or 0.2, which could be obtained for operation outside of the MELLLA region, would not be supported with sufficient counts unless the amplitude setpoint is reduced to the degree that spurious scrams become probable. A review of this situation was conducted by simulating the limiting transient of a two pump trip from the highest rod line. As provided in more detail in Section 3.3, it was demonstrated that [

] result in sufficient confirmation counts for reliable detection while the signal amplitude remains at or below the system amplitude setpoint.

The calculation of the [ ] the relationship between the setpoint and the confirmation count is provided in Appendix C. [

] It should be noted, the relation between the number of confirmation counts and the amplitude setpoint described in the Reference 2 methodology [ ]

### 3.2.2 Statistical Analysis of the Hot Channel Oscillation Amplitude

This section addresses the second segment of the oscillatory power signal interacting with the system algorithms, namely the time between the relative signal amplitude crossing the system amplitude setpoint and the time a scram successfully suppresses the oscillation. The HCOM is analyzed statistically using a Monte Carlo method similar to the method described in the LTR of Reference 2. This analysis uses typical parameter values instead of plant-specific data, and is therefore limited to addressing the relative sensitivity of HCOM to oscillation characteristics. The sensitivity to oscillation characteristics, growth ratio and period, are found to be too small to warrant a modification of the system hardware or setpoints.

#### 3.2.2.1 Effect of the Oscillation Growth Ratio

The growth ratio distribution given in Reference 2 has been scaled, using an appropriate scaling factor applied to the original distribution, to allow its biasing to higher (or lower) growth ratios. The resulting change in HCOM as a function of the scaling parameter is better represented as the effect of the scaling parameter on the system amplitude setpoint ( $S_p$ ) that would protect the core against the same HCOM. The statistical HCOM sensitivity analysis shows that increasing the oscillation growth ratio affects the hot channel oscillation magnitude at the time of suppression, which requires a decrease of the system amplitude setpoint. The magnitude of such adjustment in the setpoint due to the expected increase in oscillation magnitude is found to be small (of the order of 0.005) at the less stable conditions. Conversely, the corresponding increase in the HCOM, if the amplitude setpoint is held constant, is approximately 5%, which is small. Figure 3-6 shows these results as a calculated decrease of the amplitude setpoint due to the growth rate up-scaling. In order to appreciate the range of the growth rate sensitivity used in the analysis, the effect of the scaling parameter on the probability of sampling high growth ratios is presented in Figure 3-7, and a sample of the biased probability distributions are given in Figure 3-8. While it is true that the effect of distribution scaling on the probability of sampling low decay ratios is small, the occurrence of high growth ratios ( $>1.2$ ) which may potentially challenge the system as currently configured is the main interest. It is clear from Figure 3-7 that a substantial increase in sampling high growth ratios is achieved in the selected scaling range, which covers any anticipated destabilizing effects, e.g. due to operation in flow domains outside of the current MELLLA domain.

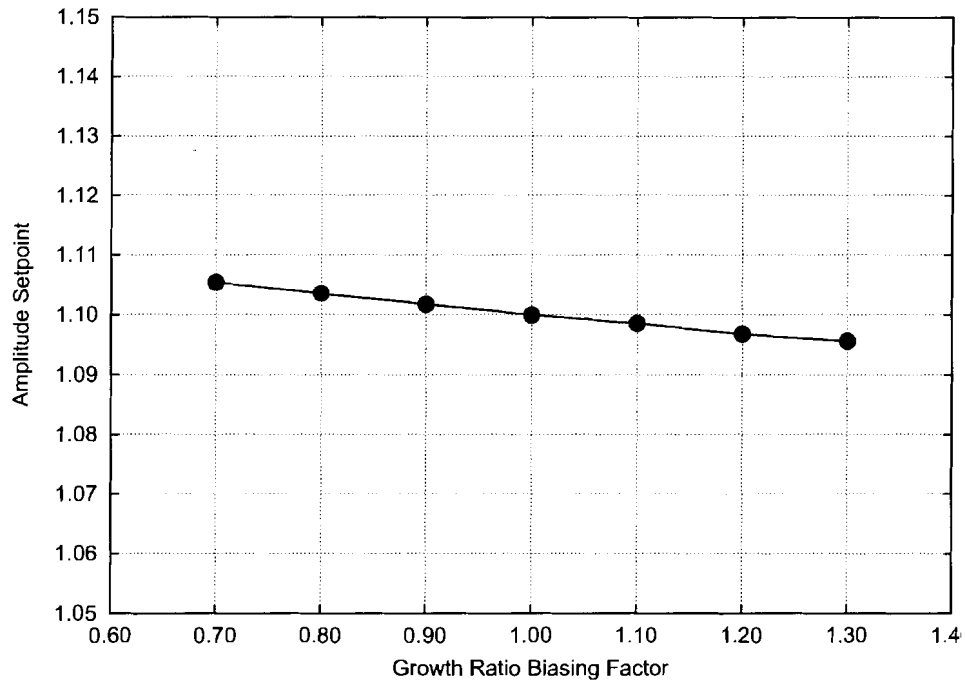


**Figure 3-6 Effect of Growth Ratio on HCOM**

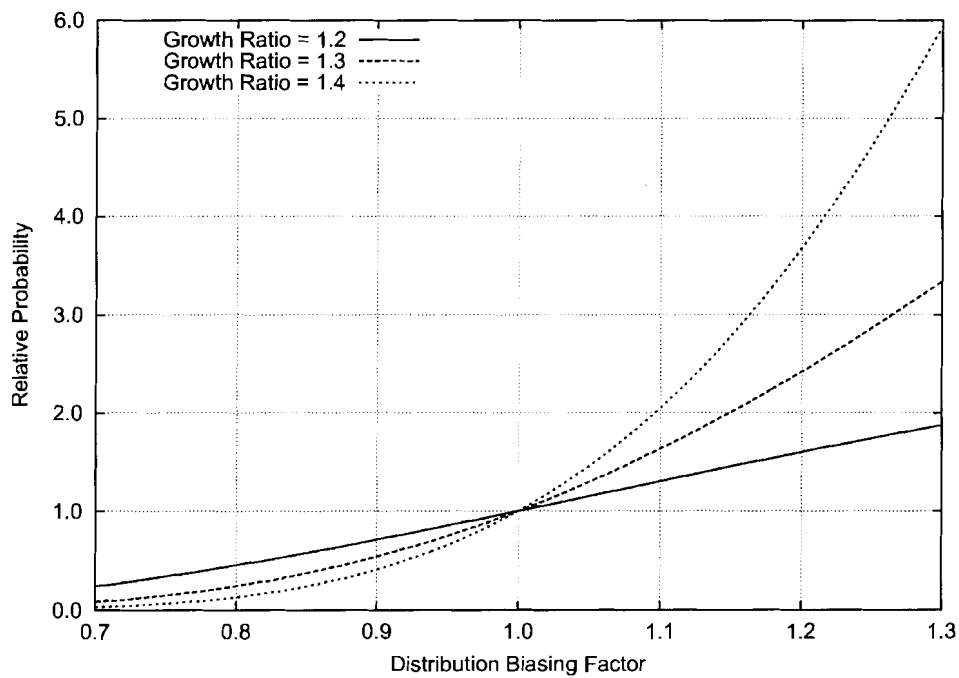


**Figure 3-7 Impact of Biasing the Growth Ratio Function on Sampling Probability**

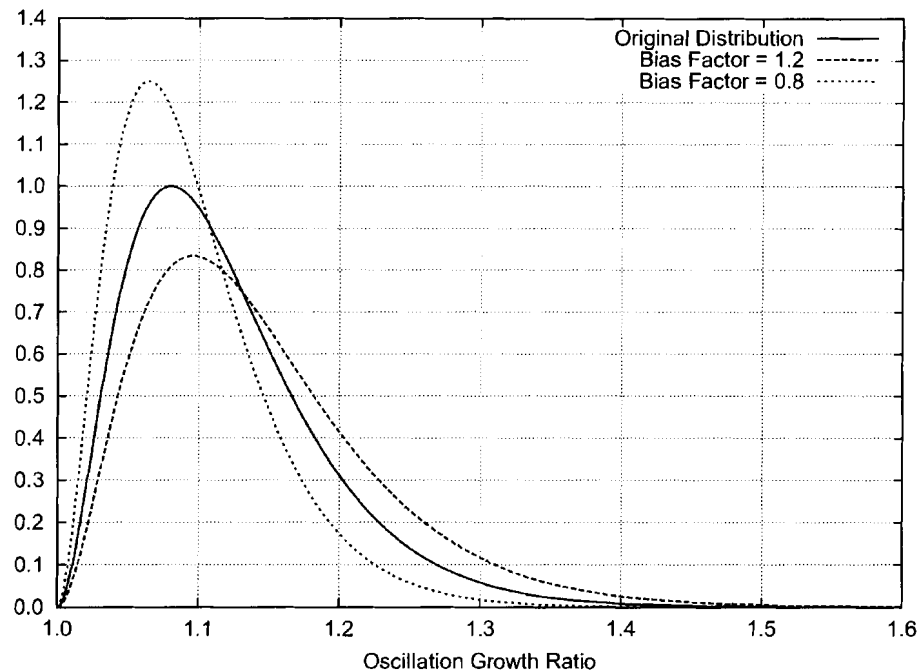


**Figure 3-8 Biased Growth Ratio Probability Functions**

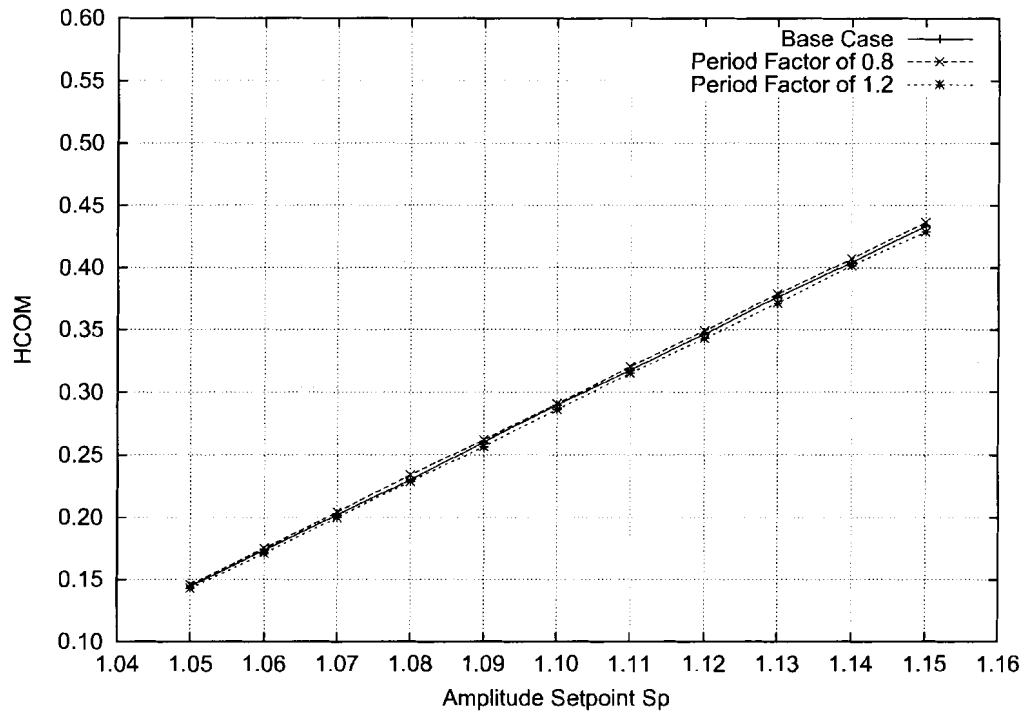
### 3.2.2.2 Effect of the Oscillation Period

The D&S algorithms use the time measured in periods. Thus, the variation of the sampled oscillation period from the distribution given in Reference 2 has a negligible impact on the calculated HCOM, except when accounting for the scram delay which is explicitly accounted for in the original HCOM methodology. As expected, the statistical analysis of the variation of HCOM due to oscillation period scaling yielded negligible sensitivity as shown in Figure 3-9.

As the scram delay, in units of oscillation periods, is increased with down-scaling the period distribution, the hot channel oscillation magnitude at the time of oscillation suppression is expected to increase. This small increase is more than compensated for by other oscillation period effects not taken into account for reasons of maintaining a high degree of conservatism

[

]

**Figure 3-9 Effect of Period on HCOM**3.3 *I*



[

]

### 3.3.1 Two-Pump-Trip Transient

Consider a BWR operating at full power and reduced flow corresponding to the highest control rod line. A two-pump trip initiates flow reduction, which results in increasing the void content in the core and produces negative reactivity.

A slow flow reduction would, by definition, take the operating point to a lower power along the control rod line. On the other hand, the flow reduction caused by the two pump trip is so fast that the power transmitted to the coolant remains high due to the fuel thermal inertia. This causes a rapid void generation and the nuclear power generation drops quickly due to the negative void reactivity. Following the initial phase of rapid power generation reduction, the power transmitted to the coolant starts to drop with a time constant of 4~5 seconds as the energy stored in the fuel is transferred to the coolant. The reduction in heat transfer to the coolant lowers the void content and the reactivity increases resulting in partial recovery of the generated power level. In this way, the operating point is brought close to, but not quite at, natural circulation and power at relatively high levels approaching the instability boundary. This stage comes to an end with an additional flow reduction due to the void reduction resulting in reducing the core pressure drop, thus bringing the operating point to natural circulation level with a time scale of the order of 10~15 seconds. The power at that point is sufficiently high and the onset of oscillations cannot be precluded. The third stage is characterized by the delayed response of the feedwater flow to the power reduction. The resulting increase in core inlet subcooling brings about two effects: (1) the void fraction is reduced further resulting in power increase, which takes the operating point deeper into the stability exclusion zone, and (2) the core is destabilized further due to the effect of increased subcooling.

Summing up, a two pump trip transient can be conceptually characterized by 3 phases with differing time frames.

1. The first phase, the tripping of the pumps and the initial flow reduction is very fast, but sufficient stability margins remain throughout this phase.
2. The second phase, where the flow approaches natural circulation and power increases due to the depletion of the energy stored in the fuel. This stage may take the core into an unstable state if the transient started at sufficiently high power, but the growth ratio characterizing the degree of instability – should one occur -- is not expected to be high. The time scale of the approach to this condition depends on the fuel thermal time constant and recirculation loop response time, and can be estimated on the order of 10~15 seconds.
3. The third phase is the final destabilization of the core due to the initial increase in core inlet subcooling, which is characterized by a time scale on the order of 15 seconds.

Now a qualitative distinction is made between the situations where the two pump trip transient is initiated at the 100% control rod line, and the case where the initial state is at a higher rod line such as the case with MELLLA+. In the case of high rod line, the final state at natural circulation is less stable due to the relatively high power. This implies that the system [

] at the asymptotic operating point unless  
suppressed by operator or automatic action.

[

]

[

]

The conceptual and qualitative aspects of the two pump trip transient [ ] described in this section are verified using a reduced order model and full system code calculations which are presented in the next two subsections.

### 3.3.2 [ 1 Reduced Order Model Results ]

A reduced order model, similar to the one presented in Section 3.1.3, is used to simulate the [ ]

]

The results are presented in Figure 3-10 where it is observed that:

- The average trajectory of the power level is the same [ ]

]

[

]



**Figure 3-10 [ ] Instigation of Oscillations  
Using the Reduced Order Model**

### 3.3.3 [

### ] RAMONA5-FA Results

Detailed simulations of a two pump trip were performed with the full system transient code RAMONA5-FA. The full system simulation includes all the aspects of the transient including the

pressure and feedwater responses as well as accurate representation of the loss of pumping head. The neutron kinetics model was also specified [

] From these detailed simulations, the same conclusions can be drawn, namely: [

]

which is anticipated to be higher for extended flow windows.

Figure 3-11 demonstrates the power/flow trajectory [ ] The power/flow is plotted for the transient period prior to significant core oscillations. In addition, constant decay ratio lines for channel decay ratios of 0.8, 0.9, and 1.0 are also included. Figure 3-11 shows that the operating state has crossed the calculated channel exclusion region prior to significant core oscillations. The core power versus time is given in Figure 3-12, and shows small initial global oscillations developing into double frequency oscillations, indicating the presence of large regional oscillations. Figure 3-13 gives the hot bundle power versus time, and shows small initial oscillations with the decay ratio eventually growing to large magnitudes. The hot bundle CPR versus time is given in Figure 3-14. The core inlet subcooling versus time is given in Figure 3-15. Finally, Figure 3-16 plots the hot bundle power for two cases, [

]

**Figure 3-11 Power Generated Versus Total Core Flow Using  
RAMONA5-FA**

**Figure 3-12 Core Power Generated Versus Time Using  
RAMONA5-FA**

**Figure 3-13 Hot Bundle Power versus Time Using RAMONA5-FA**

**Figure 3-14 Hot Bundle CPR versus Time Using RAMONA5-FA**



**Figure 3-15 Core Inlet Subcooling versus Time Using RAMONA5-FA**



**Figure 3-16 [ ] Oscillation Instigation Using RAMONA5-FA**



#### 4.0 Elements of the Enhanced Option III

The Enhanced Option III solution is made up of the core elements of the original Option III solution, with modifications in response to the need to meet the requirements for reduced stability beyond what was originally licensed. Such reduced stability is anticipated with operating schemes such as MELLLA+.

The consequences and remedial enhancement measures of anticipating higher oscillation growth ratios and deeper penetration of the instability boundary are summarized below.

- Consequence: Higher growth ratios may reduce the time available for the PBDA to generate the minimum number of period confirmations required for reliable identification of oscillatory behavior prior to the signal reaching the system amplitude setpoint.

- Remedy: [

] the number of available confirmation counts  
remains adequate for reliable detection.

- Consequence: Once the amplitude setpoint is reached, oscillations with higher growth ratios may not allow for timely suppression given the delay required to accommodate the trip logic and scram hardware.
  - Remedy: The statistical hot channel magnitude analysis was studied to quantify the effect of higher growth ratios. It was found that the effect is minor. A small penalty reduction of the amplitude setpoint on the order of 0.005 or less is sufficient to remedy the situation.
- Consequence: Deeper penetration of the instability threshold may excite multiple oscillation modes, most likely one or more hydraulic channels may become decoupled and interact with the regional mode. Should this occur, the DIVOM relationship is no longer valid, and calculated DIVOM curves depict elevated and erratic slopes.

- Remedy: Protect the single channel mode by reactor scram using a calculated exclusion zone defined on the power-flow map which is protected by reactor scram. At the same time, to be consistent with this remedial measure, the DIVOM curve calculation procedure is updated to exclude the presence of the single channel instability mode.

In summary, the new elements to be introduced as enhancements to the existing Option III solution are:

1. The introduction of a calculated exclusion zone on the power-flow map to preclude single channel instabilities, and
2. The modification of the calculation procedure to exclude single channel instabilities consistent with the exclusion zone definition.

## 5.0 Licensing Procedure

The licensing of the Enhanced Option III solution is based on a cycle specific calculation or confirmation of the validity of previous cycle calculations. The new or modified elements are given below.

### 5.1 Channel Exclusion Definition

A conservative exclusion boundary for the single channel mode is calculated based on the frequency domain code STAIF (or equivalent code). The procedure for this calculation is given below:

- The hot channel decay ratio (CHDR) protected by the exclusion zone is  $CHDR=1.0$  with appropriate accounting for code uncertainty. The channel decay ratio exclusion region boundary is thus defined by the channel stability uncertainty criterion of the code used. This exclusion region is protected by reactor scram.
- The exclusion region is defined by an appropriate number of calculated points on the power flow map corresponding to the code acceptance criterion for channel decay ratio. The exclusion region is thus defined to bound all calculated points.
  - One example is the exclusion region boundary interpolation function defined for the backup stability solution in Reference 7. This function requires two points, one at the natural circulation boundary, and one at the highest rod line.
- Best estimate calculations are performed at the following conditions
  - Constant xenon corresponding to rated power conditions
  - Feedwater at equilibrium conditions of the specific power/flow point
  - Statepoints based on the nominal current cycle target control rod step-through with appropriate allowances made to bound normal operational variations in the bundle radial peaking factor.
- The entire calculation is repeated over a variety of exposure points, and the largest exclusion region is used. These calculations should be performed for a sufficient number of exposure points to provide a bounding region to protect the entire cycle.

- If the feedwater heaters out-of-service scenario is to be supported, then the previous steps will need to be repeated using the reduced feedwater temperature.

An example of the calculated channel exclusion region is shown in Figure 5-1.

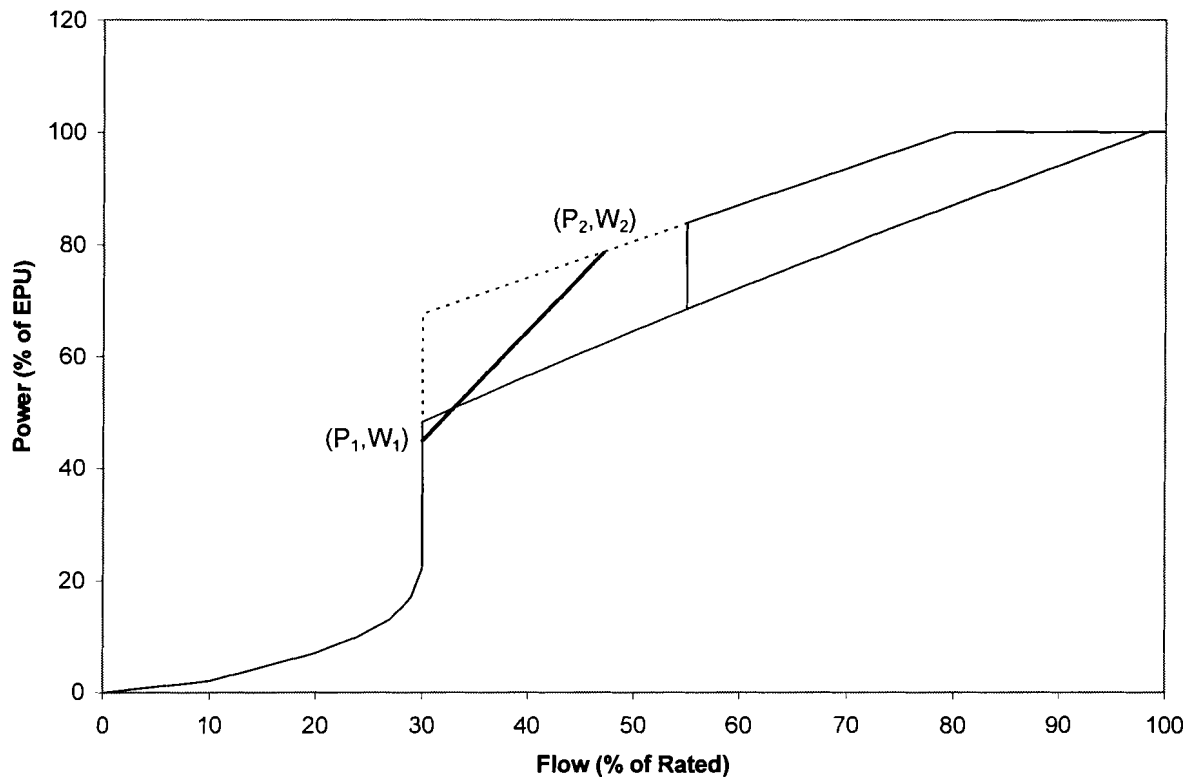


**Figure 5-1 Example Channel Exclusion Region**

## 5.2 ***DIVOM Calculation Procedure***

The time domain system code RAMONA5-FA (or equivalent code) is used for calculating regional instability transients from which DIVOM data are extracted following the procedure detailed in Reference 4. Additionally, the transient data produced by the code for any given run are examined to detect the presence of any single (or few) channel excitation components. The presence of a channel instability is manifested as an irregular DIVOM curve with elevated slope, and can be confirmed by detailed examination of the transient output. The transient analysis is performed for two points as shown in Figure 5-2.

- Point A: Corresponds to natural circulation flow, but with reduced power. The value of the power at this point,  $P_A$ , is anywhere between the highest power at natural circulation and the exclusion boundary ( $P_1, W_1$ ). The exact power in this range determined to satisfy the criteria below:
  - The power  $P_A$  should be sufficiently high to produce unstable regional oscillations
  - The power  $P_A$  should be less than the power level needed for a channel instability
  - The margin  $P_A - P_1$  serves as an additional indication of conservatism that the exclusion boundary calculated by an independent code (in this case the frequency domain code STAIF) protects against hydraulic instabilities.
- Point B: Located on the highest control rod line anywhere between the natural circulation point and the exclusion region point ( $P_2, W_2$ ). Again, the exact location of point B is determined to satisfy the following criteria:
  - Regional mode instabilities are excited
  - No single channel mode is detected

The DIVOM curve used for the cycle-specific licensing calculation of the amplitude setpoint is the most conservative curve calculated at the two points described above.

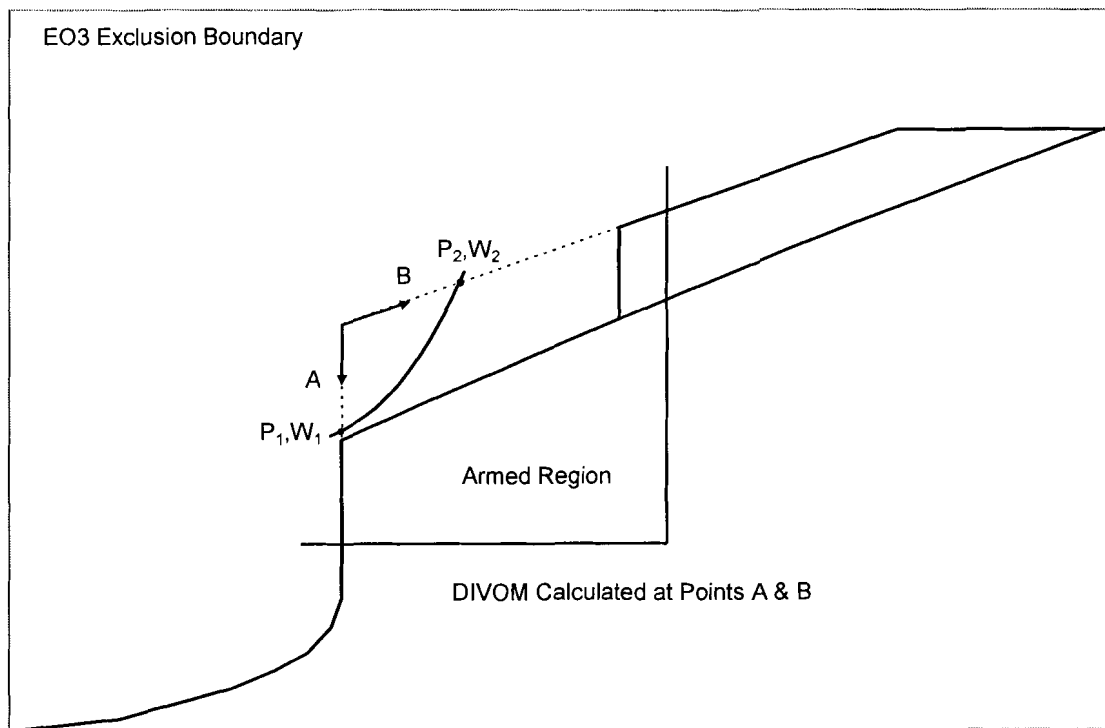


**Figure 5-2 Definition of the DIVOM Calculation Points for EO-III**

### 5.3 ***Pre-Oscillation MCPR***

Section 4.2 of Reference 2 describes the calculation procedure used to calculate the pre-oscillation initial MCPR (IMCPR). The calculation calls for two separate values of IMCPR, one corresponding to a two pump trip from rated power along the highest rod line to natural circulation flow. It is assumed that the reactor is operating at the MCPR Operating Limit (MCPROL) prior to the two recirculation pump trip. The second scenario corresponds to steady-state operation at 45% core flow at the highest rated rod line. It is assumed that the reactor is operating at the MCPROL corresponding to the specified power and flow conditions. For Enhanced Option III, this calculation is split into two sets, consistent with the changes to the DIVOM calculation procedure.

The first set of calculations are performed at the highest rod line, and consist of a simulation of a flow runback from rated power along the highest rod line to the point of intersection between the highest rod line, and the channel exclusion region ( $P_2, W_2$ ) from Figure 5-2. The second point in this set corresponds to steady-state operation at 45% of rated core flow at the highest rod line.

If the channel exclusion region intersects the highest rated rod line at a flow greater than 45%, then this point will be performed at the point corresponding to the intersection of the channel exclusion region and the highest rated rod line from Figure 5-2.

The second set of calculations is performed at the rod line corresponding to the intersection of the channel instability region with the natural circulation line ( $P_1$ ,  $W_1$ ) from Figure 5-2. The calculation will be performed for a two pump trip from rated power along the rod line intersecting point ( $P_1$ ,  $W_1$ ).

#### 5.4 ***Amplitude Setpoint Analysis Modification***

The plant-specific HCOM analysis results, which are required for the cycle-specific licensing analysis of the system amplitude setpoint, provide a table of HCOM versus Sp. The Enhanced Option III solution introduces a conservative adjustment of the HCOM value by +5% in order to account for increased oscillation growth ratio anticipated from extended flow windows.

#### 5.5 ***Identification of Conservatisms in the Licensing Basis***

A summary of the conservative selection of the new parameters introduced for the Enhanced Option III is discussed in this section.

- Channel instability exclusion region is conservative. [

]

Given the high level of accuracy of the frequency domain code STAIF, as shown by its benchmark database against 94 test data points plotted in Figure 5-3, an estimated uncertainty of the STAIF channel decay ratio of [

]

- Calculations with STAIF & RAMONA5-FA confirm the exclusion region conservatism. Figure 5-4 provides comparison of RAMONA5-FA predicted versus measured channel

decay ratios which shows good agreement. The two codes, using different methods, effectively produce two exclusion region boundaries. The boundary defined by the interpolation function connecting the Points (1) and (2) is produced by the frequency domain code STAIF, while an effective boundary is created by the points (A) and (B) for which the time domain code RAMONA5-FA calculates DIVOM transients while confirming the absence of single channel instabilities. The margin between the two exclusion boundaries constitutes a measure of conservatism in the methodology.

- The HCOM penalty of +5% is added to the already conservative Monte Carlo analysis of the system performance to account for increased oscillation growth ratios for extended flow windows. However, the inclusion of a channel exclusion region inherently limits the maximum core decay ratio that can be obtained. Thus, the penalties, and evaluations done to address an increase in growth rates are conservative with respect to the stable channel operating domain.

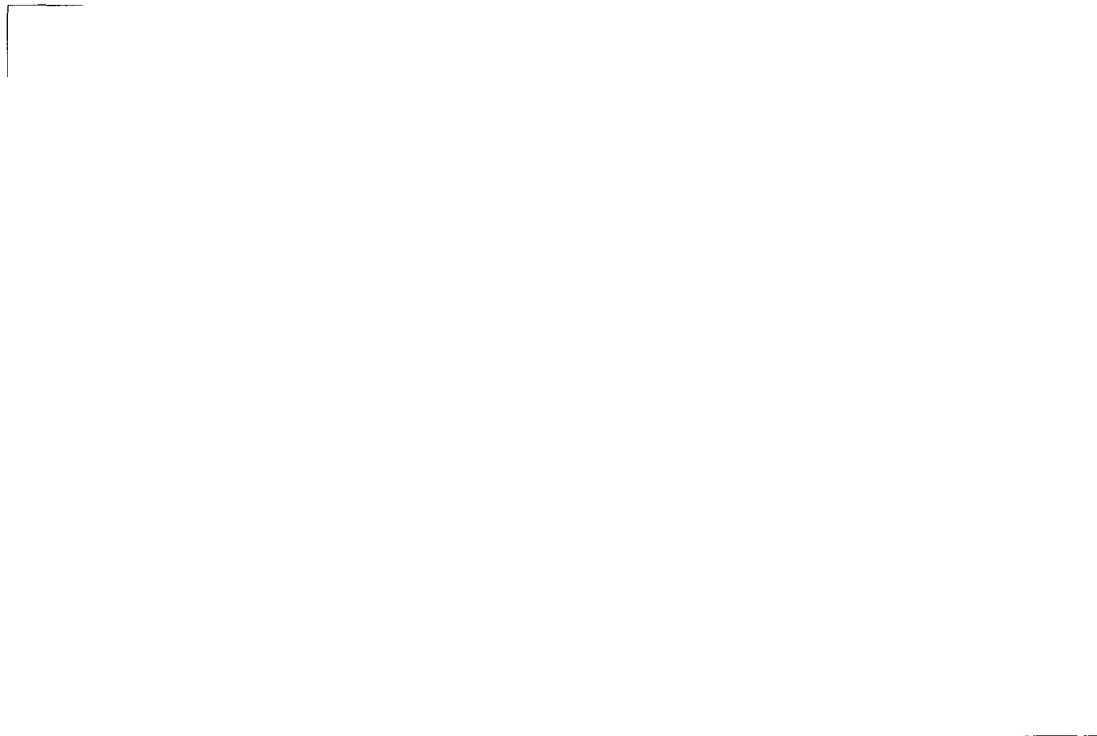


**Figure 5-3 STAIF Predicted versus Measured Channel Decay Ratio  
all Benchmark Tests**





**Figure 5-4 RAMONA5-FA Predicted versus Measured Channel Decay Ratio for ATRIUM™-10 Tests**

### 5.6 *Applicable Plant Operating Modes*

The Enhanced Option III Solution is applicable for the normal operating and licensing envelope for current BWRs, and applicable to the original Option III solution. In addition to the current licensing envelope, the Enhanced Option III Solution is also applicable for expanded flow windows. This includes:

- Normal operating power/flow operating maps. This includes lower flows up to the Maximum Extended Load Line Limit Analysis / Maximum Extended Operating Domain (MELLLA/MEOD) operating boundaries and higher flows up to the Increased Core Flow boundaries.
- Extended flow windows corresponding to control rod line defined at 80% of rated flow at an EPU power level of 120% of original licensed thermal power. This range represents the range over which the current codes and assumptions have been exercised.

Application of the Enhanced Option III solution to flow windows beyond this range will

---

\* ATRIUM is a trademark of Framatome ANP, Inc.

need to be evaluated and reviewed by the USNRC for its impact on the solution assumptions.

- Normal Equipment Out-Of-Service (EOOS) options:
  - Single Loop Operation (SLO) is acceptable since the licensing basis is protecting against regional mode oscillations which are not sensitive to the recirculation system modeling. Furthermore, the SLMCPR for SLO includes adjustments to account for the increased flow uncertainty and LPRM noise inherent in SLO.
  - Recirculation Pump Trip and Turbine Bypass Valve Out-Of-Service (OOS), or other EOOS options used to mitigate the delta-CPR response during fast-pressurization events. These systems have no effect on the operation of the OPRM system.
  - Feedwater Heater Out-Of-Service (FHOOS) and Final Feedwater Temperature Reduction (FFTR) involve taking feedwater heaters off-line with a resulting decrease in feedwater temperature and increase in core inlet subcooling. The effect of the increase in inlet subcooling is a potential increase in the channel exclusion boundary, the effects of which need to be examined in licensing analyses.

## 5.7 **Sample Plant Calculations**

A sample calculation is provided to illustrate the calculation process. The example plant is a 764 bundle BWR-4. It should be noted that the values used are reasonably assumed values, and the results are provided purely for demonstration purposes.

The exclusion region was calculated using STAIF and the applicable channel decay ratio code acceptance criterion. This exclusion region was developed using the nominal current cycle target control rod step-through using a number of exposure points. The boundary was established to bound the most limiting exposure points, with extra conservatism to bound an increase in the limiting radial bundle power of ~5% from the target step-through. An example exclusion region boundary can be found in Figure 5-1.

The sample plant uses an LPRM arrangement using 4 LPRMs in a 4P LPRM assignment. For an amplitude setpoint of 1.10, the hot bundle oscillation magnitude value is assumed to be:

$$(P-M)/A_{95/95}=0.316$$

The calculated cycle-specific DIVOM results for points A (calculated at ~3% power above the exclusion region at natural circulation) and B (calculated at a flow ~3% inside the exclusion region along the MELLLA+ line) is assumed to be bounded by a slope of 0.40 and 0.45 respectively. Therefore, the limiting DIVOM slope of 0.45 will be used. Assuming that the reactor was operating at the operating limit MCPR at rated EPU power, the IMCPR values are calculated along two rod lines. The first rod line is defined by the intersection of the exclusion region and the natural circulation line,  $(P_1, W_1)$  identified in Figure 5-1. The limiting initial MCPR is determined by the intersection of the highest rod line and the channel exclusion region,  $(P_2, W_2)$  identified in Figure 5-1, and is assumed to be 1.32. The SLMCPR is assumed to be 1.08. Thus, the final MCPR is:

$$\begin{aligned} FMCPR &= IMCPR - IMCPR * (\Delta CPR / IMCPR) \\ &= 1.32 - 1.32 * (0.316 * 0.45) \\ &= 1.13 \end{aligned}$$

This demonstrates that the amplitude setpoint value of 1.10 is acceptable.

## 6.0 References

1. J. S. Post (GE), and D. B. Townsend (BWROG), "Licensing Topical Report Reactor Stability Long-Term Solution: Enhanced Option I-A," -- Licensing Topical Report," GE Nuclear Energy, NEDO-32339-A (April 1998).
2. C. R. Lehmann (PP&L), M. P. LeFrancois (Yankee Atomic), W. R. Mertz (Southern Nuclear), Hung Le (GE), and Jason Post (GE), "Reactor Stability Detect and Suppress Solutions Licensing Basis Methodology for Reload Applications --- Licensing Topical Report," GE Nuclear Energy, NEDO-32465-A (August 1996).
3. Letter, J. S. Post (GE) to Document Control Desk United States Nuclear Regulatory Commission, "Stability Reload Licensing Calculations Using Generic DIVOM Curve," August 31, 2001.
4. BAW-10255(P) Revision 2, *Cycle-Specific DIVOM Methodology Using the RAMONA5-FA Code*, January 2006.
5. Presentation to USNRC by Mike May (Exelon Corp.), "Stability Option III DIVOM Part 21 Closure Plan," August 15, 2003.
6. EMF-CC-074(P)(A) Volume 4 Revision 0, *BWR Stability Analysis – Assessment of STAI/F with Input from MICROBURN-B2*, Siemens Power Corporation, August 2000.
7. Letter, Alan Chung (GE) to BWR Owner's Group Detect and Suppress II Committee, "Backup Stability Protection (BSP) for Inoperable Option III Solution," OG02-0119-260, July 17, 2002.

## **Appendix A Results of Interacting Regional and Channel Modes using a Reduced Order Model**

The reduced order model was fit to the state of an actual large BWR plant undergoing unstable regional oscillations during a stability test. The results of STAIF simulation with 38 channel groups were used to reproduce the linear behavior. Nonlinear thermal-hydraulic corrections were introduced and varied parametrically in several steps from zero (linear limit where hydraulic instabilities can grow without limit) to a high value at which oscillations are nonlinearly damped and barely reach sufficient magnitude necessary to construct a DIVOM curve.

Two sets of calculations were performed, one with a regional decay ratio of 1.1, and the other with a regional decay ratio of 1.2. For each set, the hot channel decay ratio was varied in several steps from 0.7 to a value exceeding the regional decay ratio. For each of these calculations, the magnitude of the thermal-hydraulic nonlinear effect was varied. A total of 552 runs were analyzed and the results are summarized below.

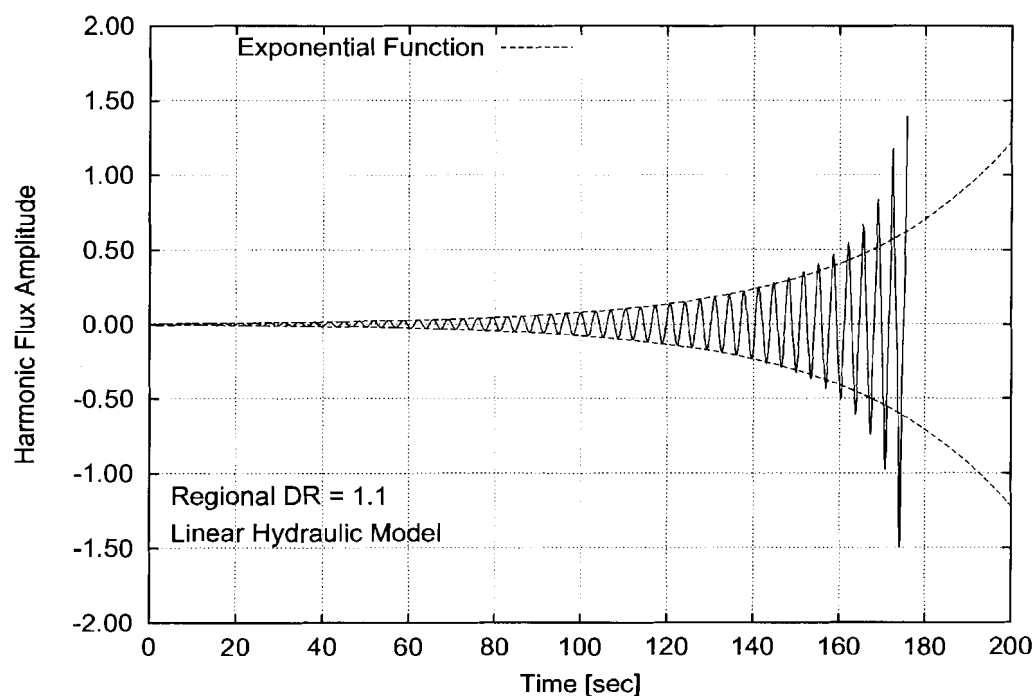
- The magnitude of the hydraulic nonlinearity has a strong effect on the time evolution of a regional oscillation. In the absence of this nonlinear term, an unstable regional oscillation is not self-limiting and does not reach a limit cycle like global mode oscillations. Figure A-1 shows that the flux harmonic amplitude growth is initially exponential with a decay ratio (DR)=1.1, and then accelerates as the oscillation magnitude increases. With an increased magnitude of the nonlinear hydraulic term, Figure A-2 shows the development of limit cycles for the case of DR=1.1. Notice that the actual flux is the sum of the fundamental and the harmonics, which is shown in Figure A-3 and Figure A-4 to have the familiar characteristics of a growing and self-limiting power oscillation.
- The level of nonlinearity is demonstrated to have no effect on the DIVOM relationship provided that the hot channel is stable. Figure A-5 demonstrates this fact for the case of channel DR=0.9 where the linear DIVOM line coincides with the one with maximum nonlinearity (the only difference is that the nonlinear oscillation amplitude range was limited by the development of a limit cycle). The same behavior is observed in Figure A-6 with a channel DR=0.99. The entire data set was plotted for all regional

decay ratios and nonlinearity levels and channel decay ratios at or below unity (stable) in Figure A-7 demonstrating that the DIVOM curve is fairly linear and well-behaved.

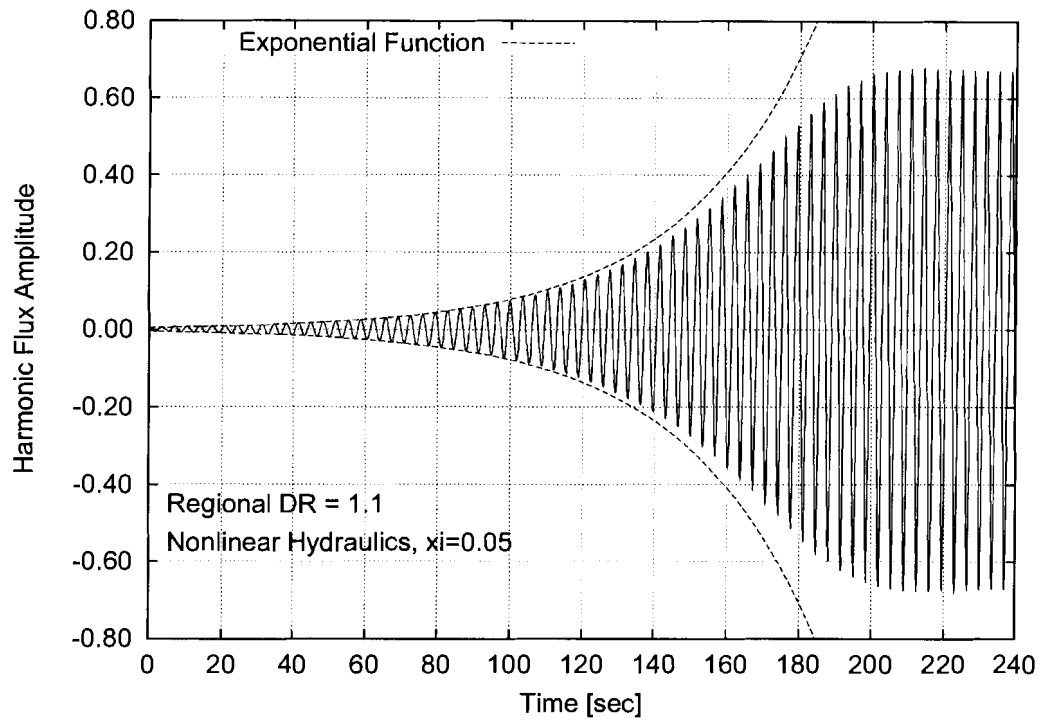
- For channel decay ratios exceeding unity, Figure A-8 through Figure A-12 show DIVOM curves with channel decay ratios from 1.04 to 1.12 which display an increasing departure from linearity due to the superposition of the self-sustained channel instability component and the component driven by the power oscillation which are generally of different frequency. A weighted average slope is constructed from the DIVOM data and the slope is found to increase dramatically when the channel is destabilized (Figure A-13 and Figure A-14). [

]

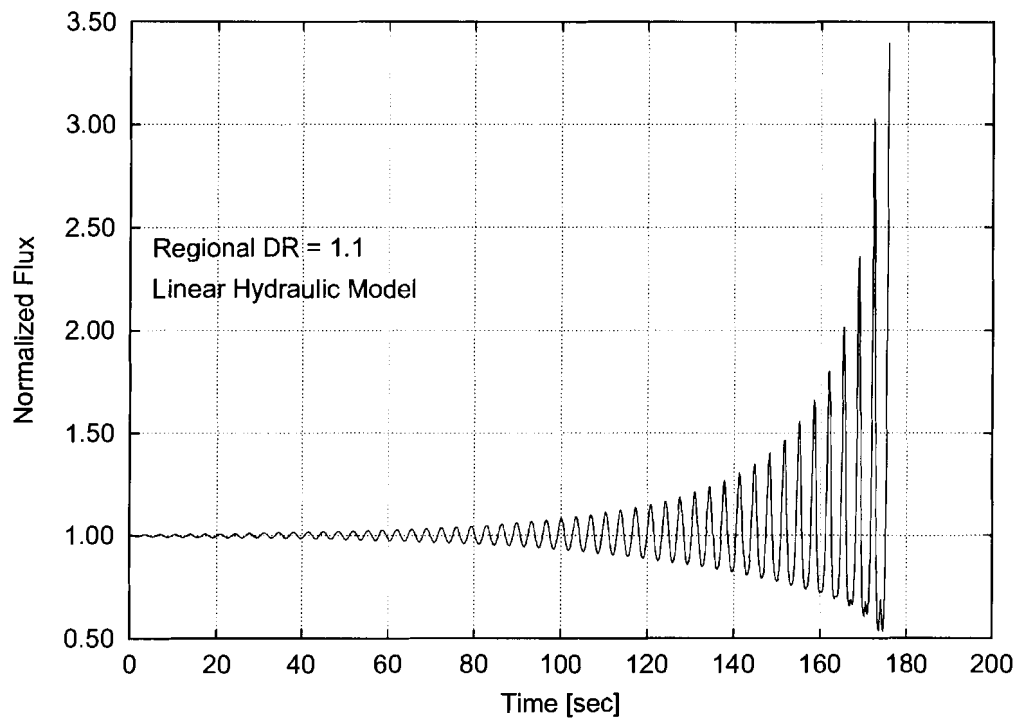
Similar calculations were performed based on a 764 bundle core, and similar results were observed as demonstrated in Figure A-15. Furthermore, the observation of the pattern and effects of interacting neutron-coupled and channel instabilities were found to be applicable to both regional and global mode oscillations.



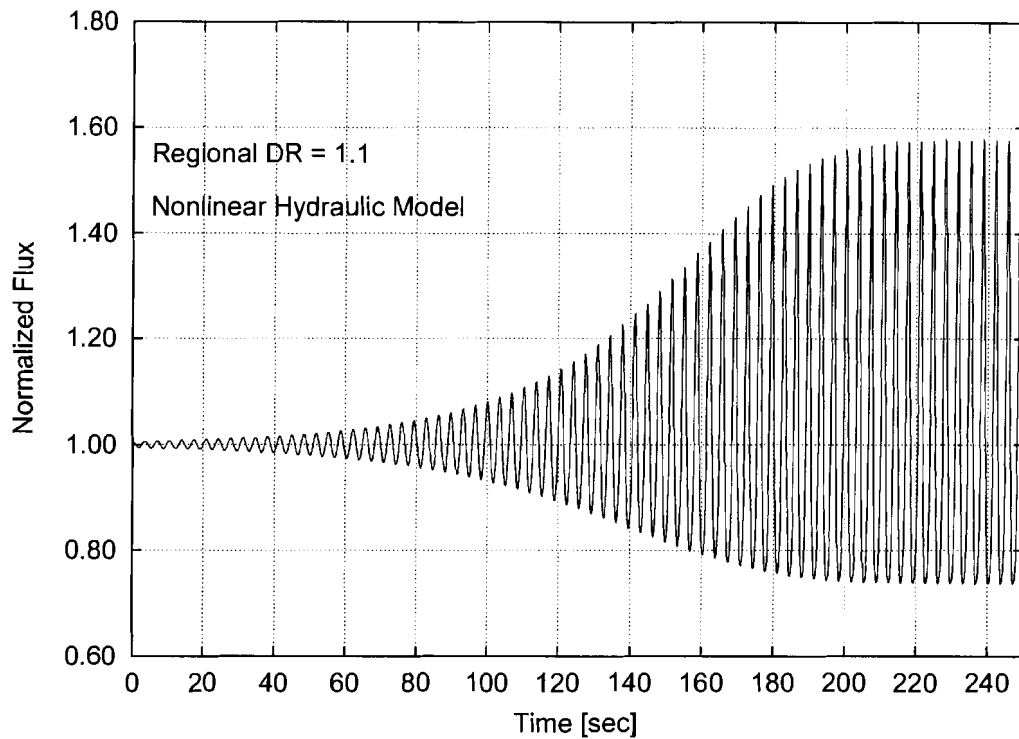
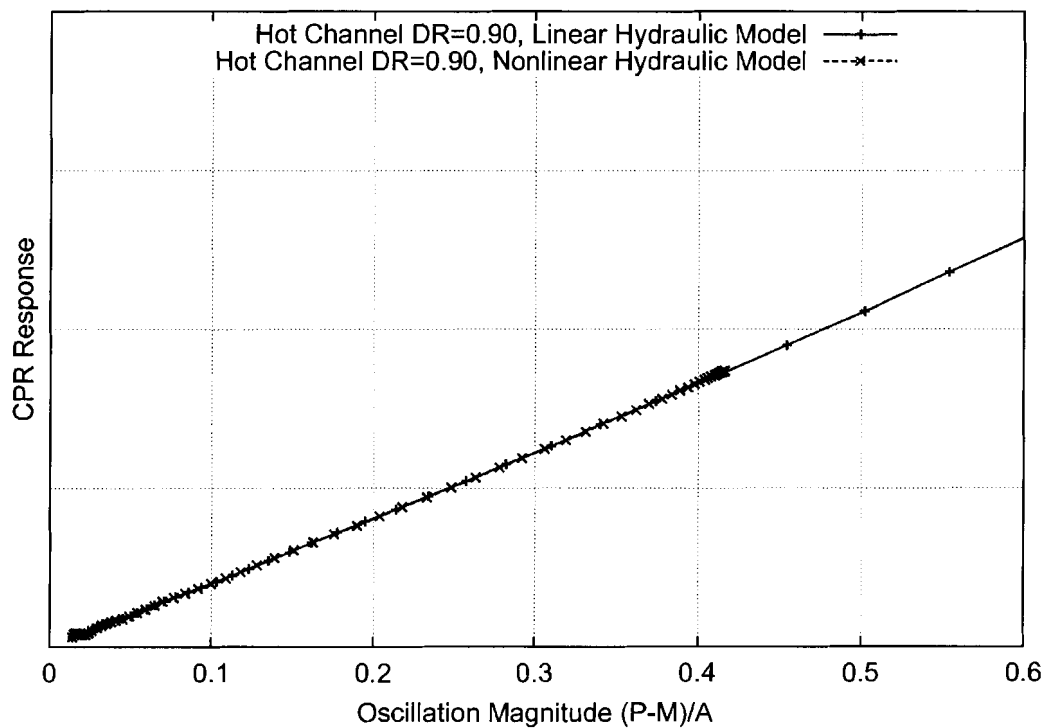
**Figure A-1 Flux Harmonic Growth Using a Linear Hydraulic Model with Regional Decay Ratio of 1.1**



**Figure A-2 Flux Harmonic Growth to a Limit Cycle Using a Nonlinear Hydraulic Model Regional Decay Ratio of 1.1**



**Figure A-3 Neutron Flux Oscillations Using a Linear Hydraulic Model**

**Figure A-4 Neutron Flux Oscillations Using a Nonlinear Hydraulic Model****Figure A-5 DIVOM Curve with a Hot Channel Decay Ratio of 0.90**



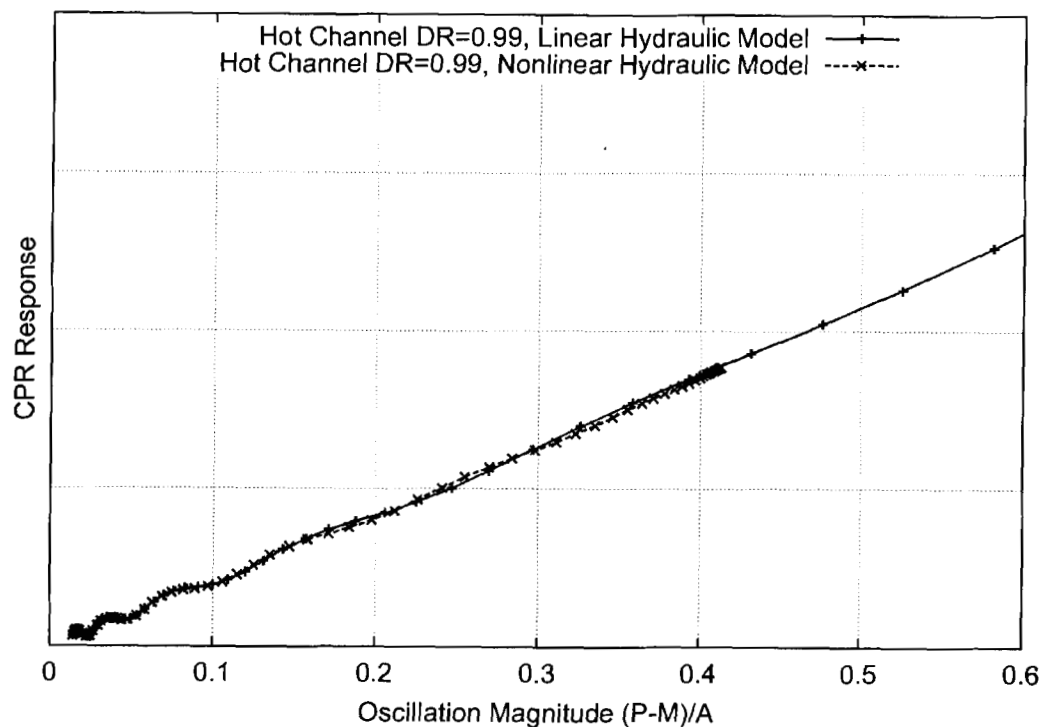


**Figure A-6 DIVOM Curve with a Hot Channel Decay Ratio of 0.99**

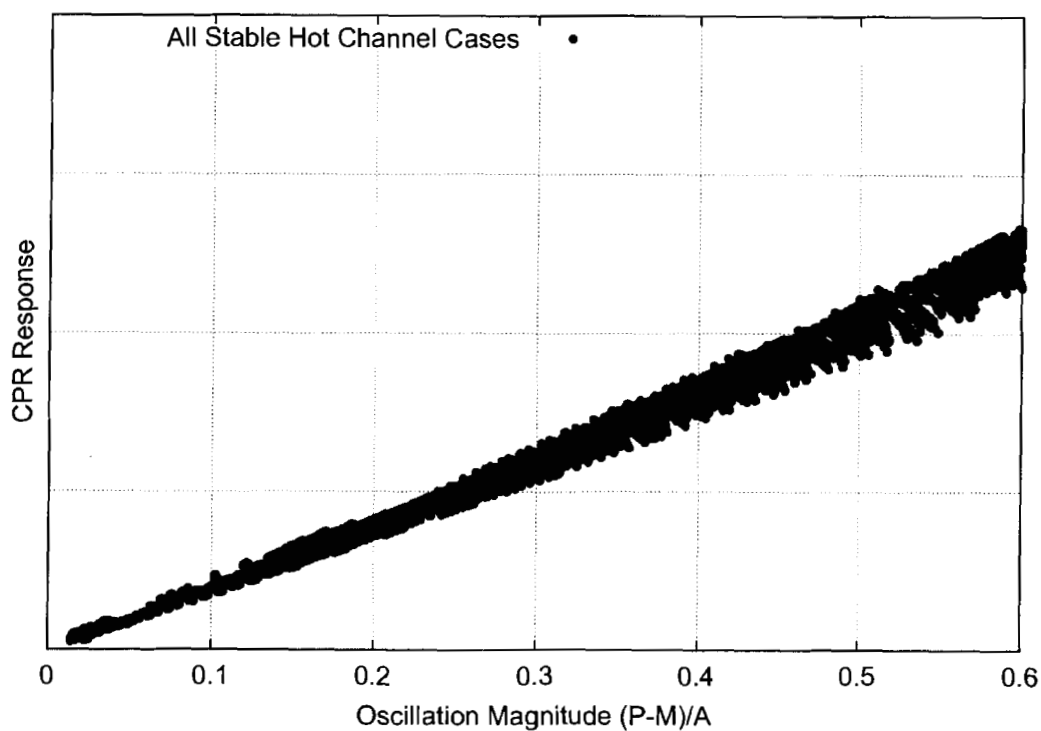


**Figure A-7 DIVOM Points for Stable Channel Cases with Varying Nonlinearity**

**Figure A-8 DIVOM Curve with a Hot Channel Decay Ratio of 1.04**

**Figure A-9 DIVOM Curve with a Hot Channel Decay Ratio of 1.06**

**Figure A-10 DIVOM Curve with a Hot Channel Decay Ratio of 1.08**

**Figure A-11 DIVOM Curve with a Hot Channel Decay Ratio of 1.10**

**Figure A-12 DIVOM Curve with a Hot Channel Decay Ratio of 1.12**

**Figure A-13 DIVOM Slope Elevation versus Hot Channel Decay Ratio for Regional Decay Ratio of 1.1**

**Figure A-14 DIVOM Slope Elevation versus Hot Channel Decay Ratio for Regional  
Decay Ratio of 1.2**

**Figure A-15 DIVOM Slope Elevation versus Hot Channel Decay Ratio for Regional  
Decay Ratio of 1.126**

**Appendix B Results of Interacting Regional and Channel Modes using RAMONA5-FA**

Two sets of calculations were performed to generate actual DIVOM data with full simulation detail (one hydraulic and one nuclear channel per bundle) using RAMONA5-FA. These two sets bracket the two interesting situations encountered when a single channel is hydraulically destabilized. One set includes a hot (unstable) channel located near the eye of the harmonic contour, and therefore subjected to maximum power oscillation driving its hydraulic response. The other set places the hot channel near the neutral line, thus minimizing the driving power oscillation and focuses on the component of self-sustained hydraulic oscillation and its effect on distorting the DIVOM relationship. The cases of symmetric cores where a pair of such channels, or when a few channels are unstable, are covered as the DIVOM distortion is dominated by the least stable channel.

Each configuration was simulated with a number of initial perturbation combinations with varying fundamental and harmonic component magnitudes. First, a sample DIVOM with no unstable channels is presented in Figure B-1. Next, a representative set of DIVOM curves are shown in Figure B-2 through Figure B-8 for the first set with the unstable channel located in the harmonic eye, and in Figure B-9 through Figure B-14 for the set where the unstable channel is located near the neutral line. The following observations are made.

- DIVOM curves for cores where all channels are hydraulically stable are invariant when the initial perturbation is varied. By contrast, when the channel is destabilized, the DIVOM relationship is different under different initial perturbations that provide different initial excitation to the core and single channel modes. The sensitivity to initial perturbation is maximum when the self-sustained channel oscillation component is dominant (channel located near the neutral line), and is relatively reduced for the case where power driven channel oscillation component is present (channel located near the harmonic eye).
- The DIVOM distortion and slope increase are evident in the cases with unstable channels regardless of their location.
- Table B-1 provides a summary of the DIVOM slopes for the first set with the hot channel located in the harmonic eye, and

- Table B-2 provides the DIVOM slopes for the second set with the hot channel located near the neutral line to demonstrate these observations.

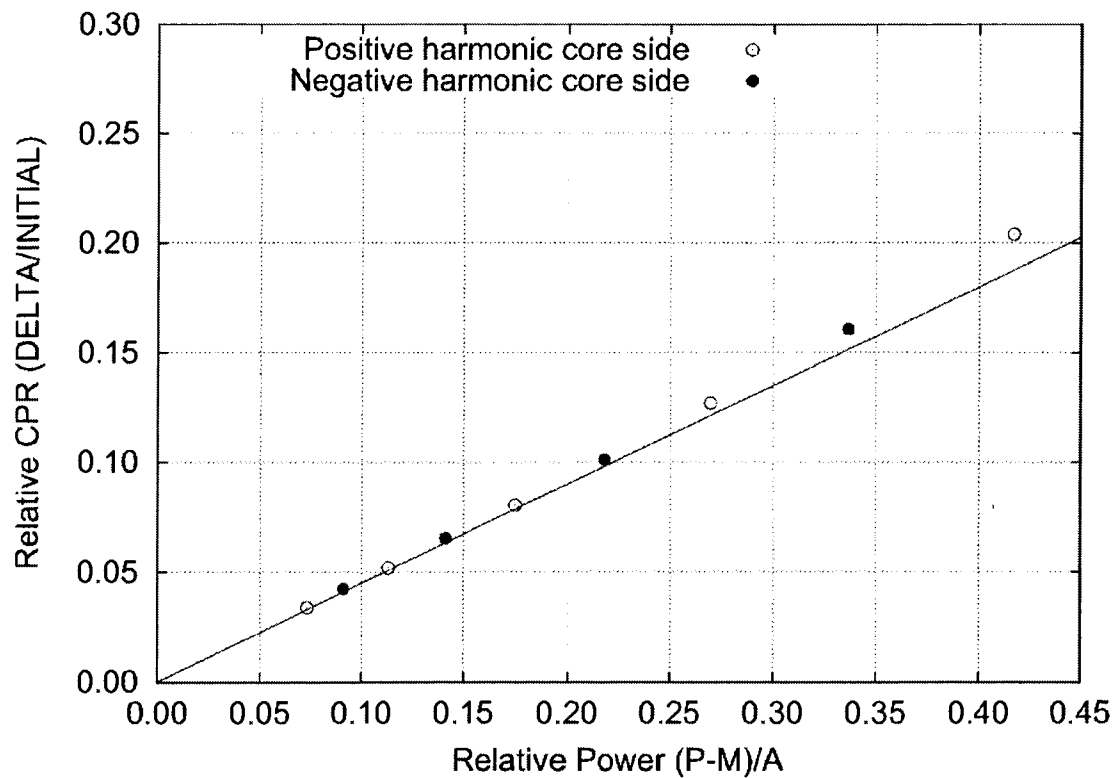


**Figure B-1 Example DIVOM Curve with No Single Channel Instabilities**

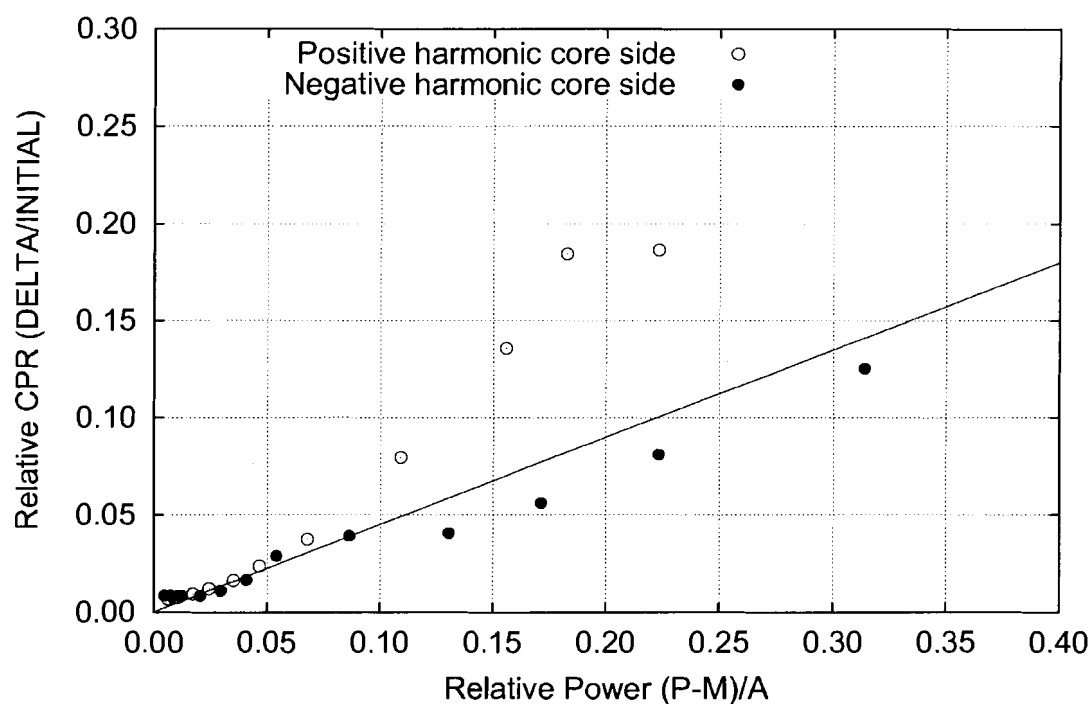


**Figure B-2 DIVOM Curve with Unstable Channel in the Harmonic Eye, 0.5% Regional, 0.0% Global Perturbation**

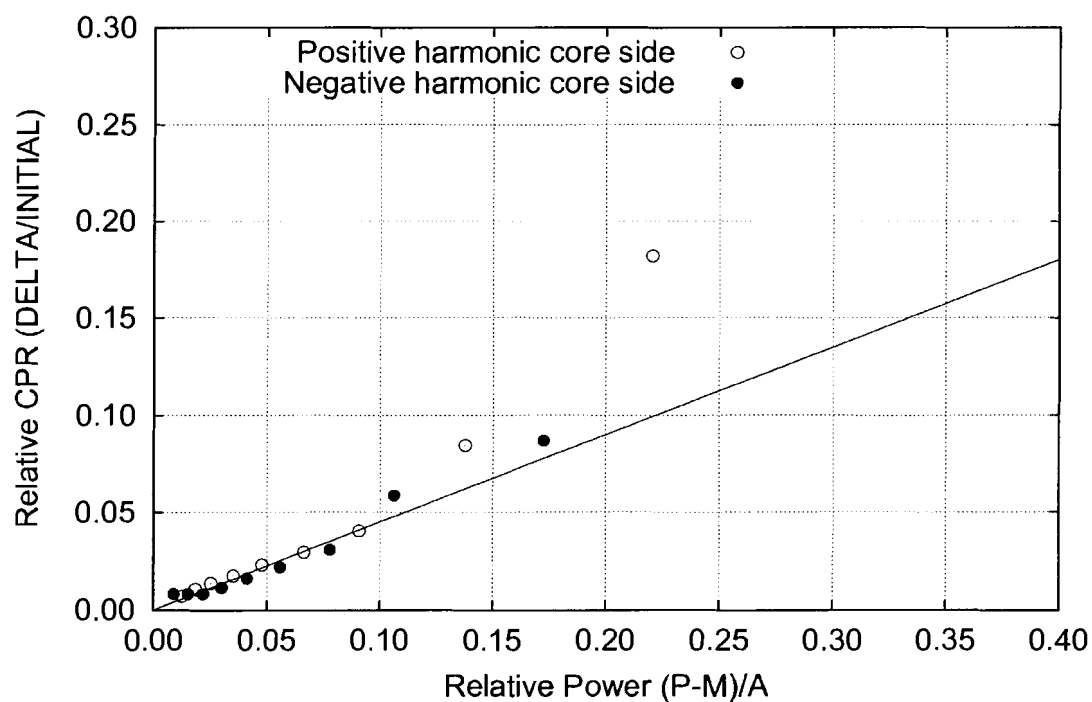


**Figure B-3 DIVOM Curve with Unstable Channel in the Harmonic Eye, 1.0% Regional, 0.0% Global Perturbation**



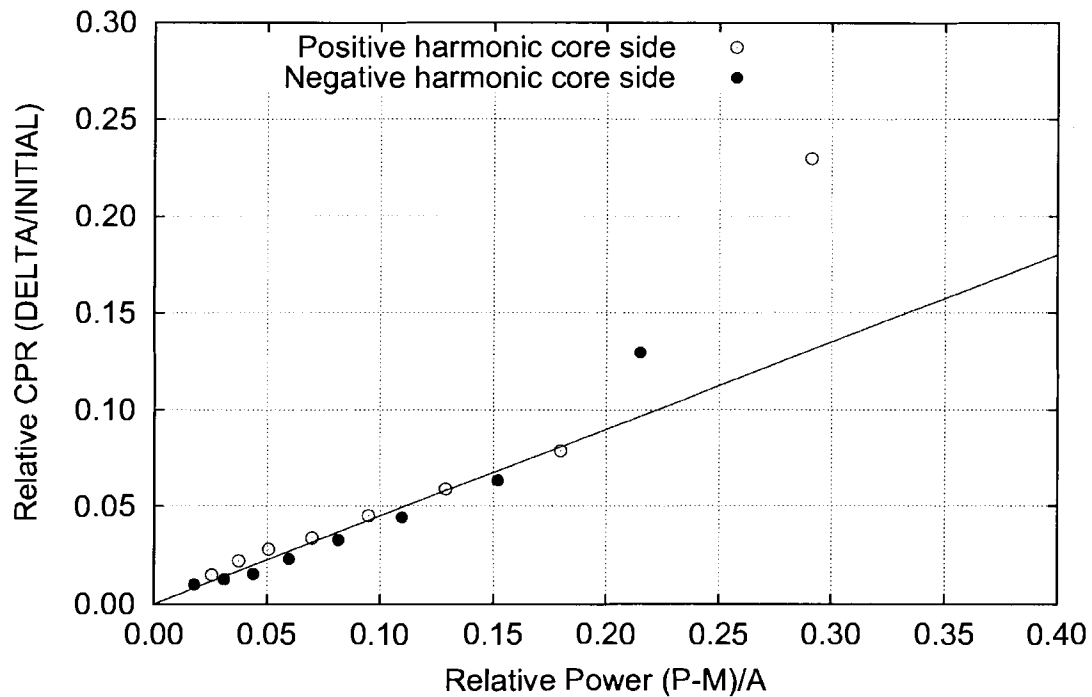


**Figure B-4 DIVOM Curve with Unstable Channel in the Harmonic Eye, 2.0% Regional, 0.0% Global Perturbation**

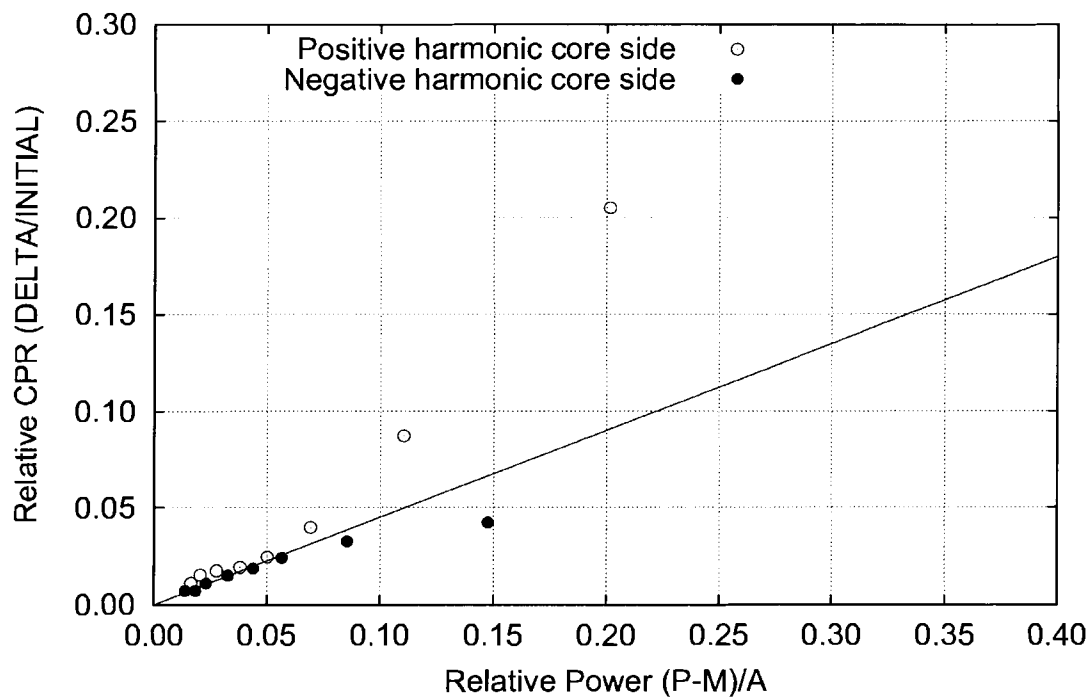


**Figure B-5 DIVOM Curve with Unstable Channel in the Harmonic Eye, 1.0% Regional, 1.0% Global Perturbation**

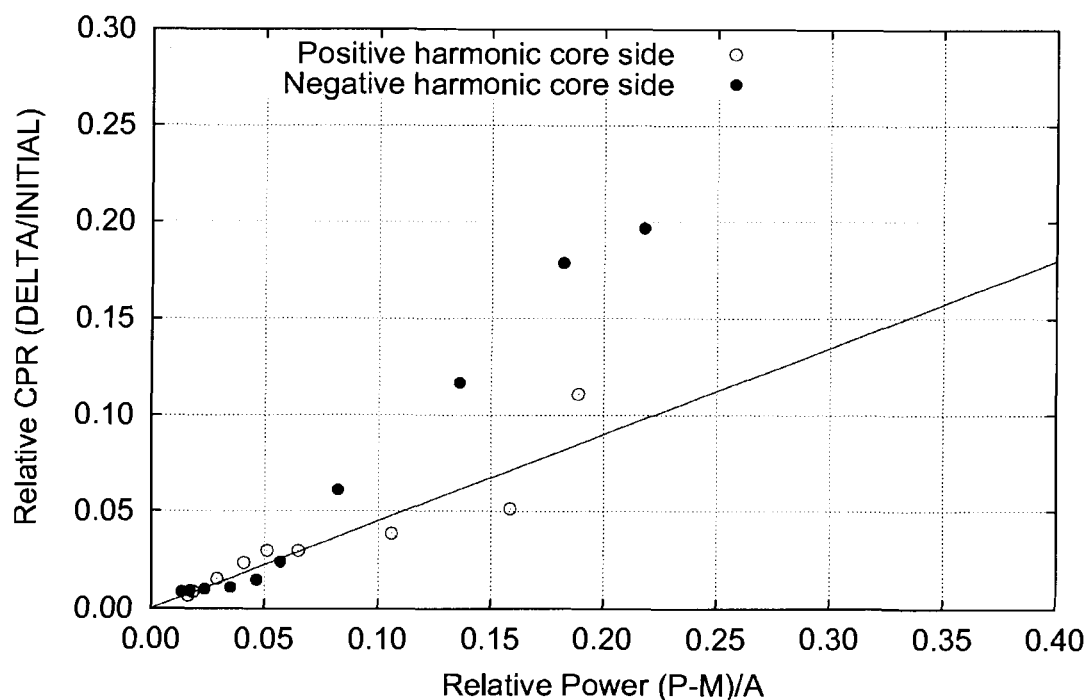


**Figure B-6 DIVOM Curve with Unstable Channel in the Harmonic Eye, 1.0% Regional, -1.0% Global Perturbation**

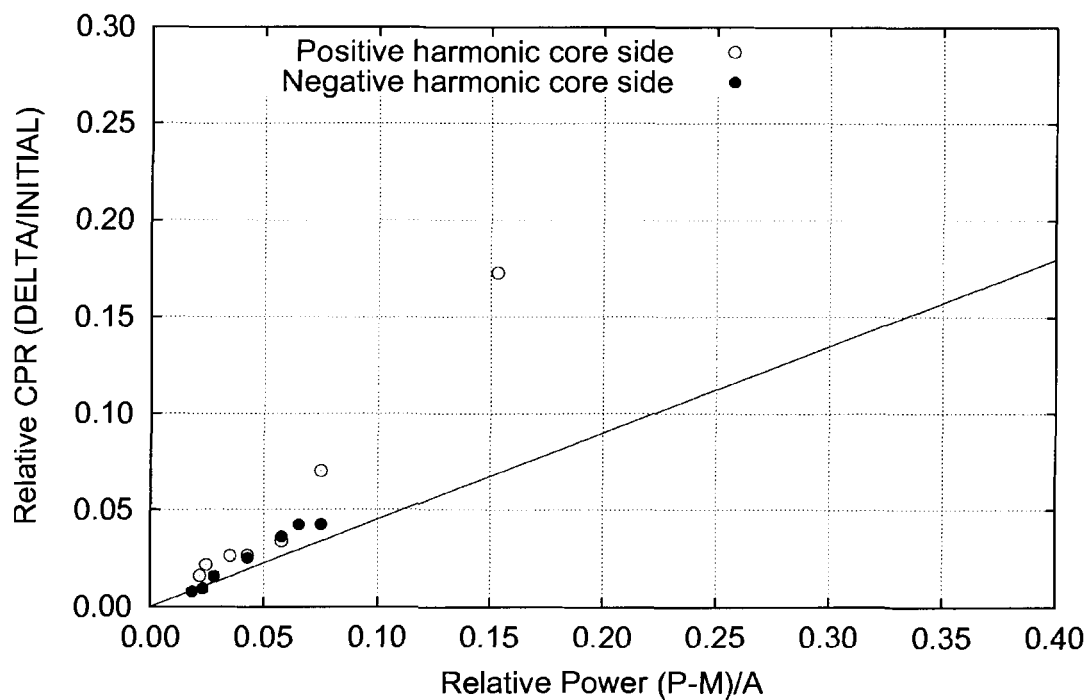


**Figure B-7 DIVOM Curve with Unstable Channel in the Harmonic Eye, 1.0% Regional, 2.0% Global Perturbation**

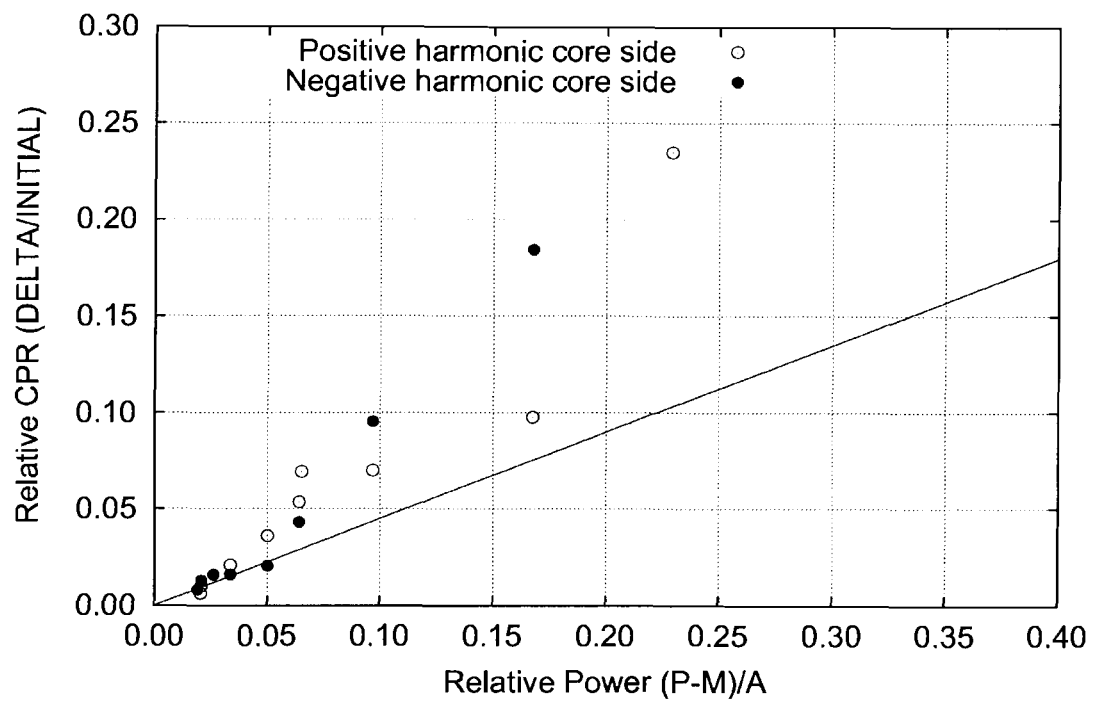


**Figure B-8 DIVOM Curve with Unstable Channel in the Harmonic Eye, 1.0% Regional, -2.0% Global Perturbation**

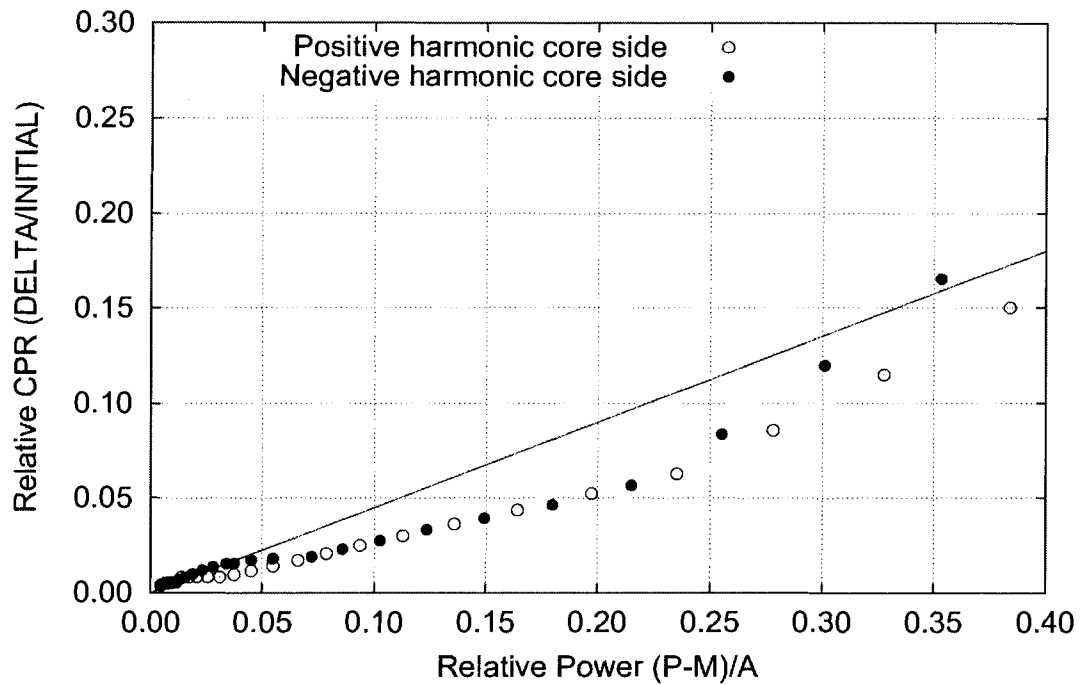


**Figure B-9 DIVOM Curve with Unstable Channel near the Neutral Line, 0.5% Regional, 0.0% Global Perturbation**

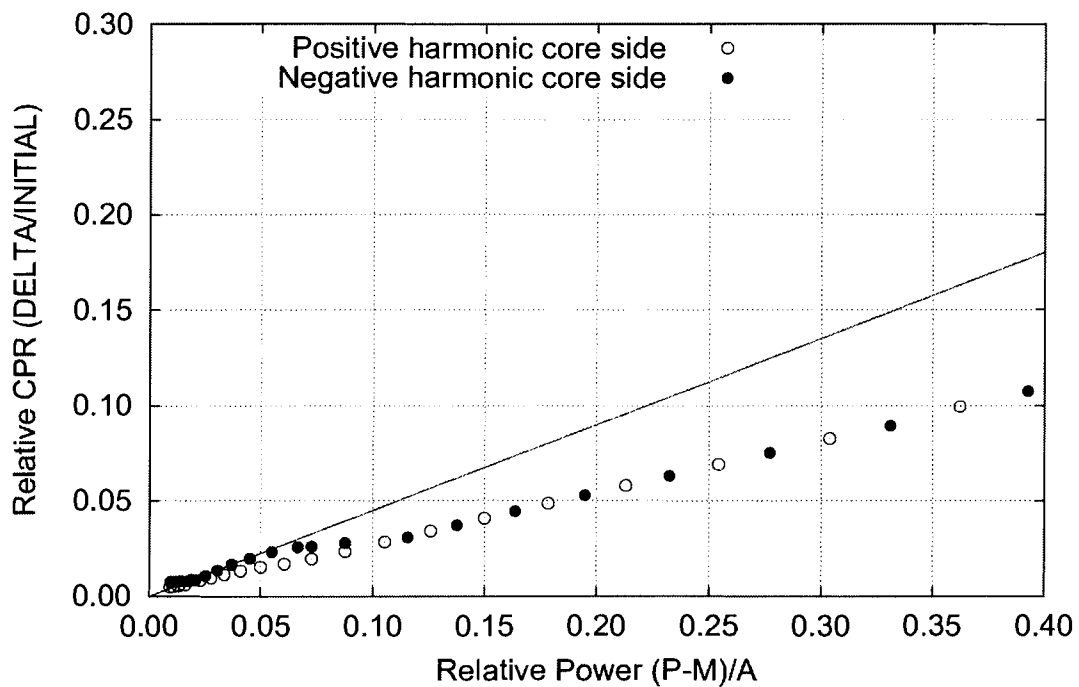


**Figure B-10 DIVOM Curve with Unstable Channel near the Neutral Line, 1.0% Regional, 0.0% Global Perturbation**

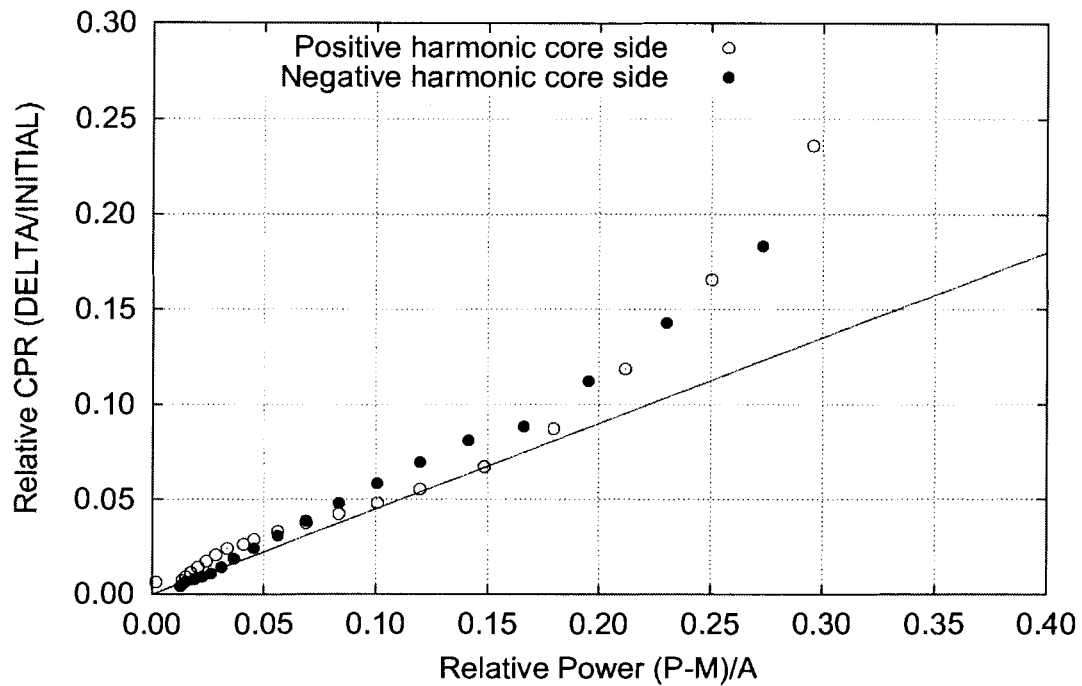


**Figure B-11 DIVOM Curve with Unstable Channel near the Neutral Line, 1.0% Regional, 1.0% Global Perturbation**

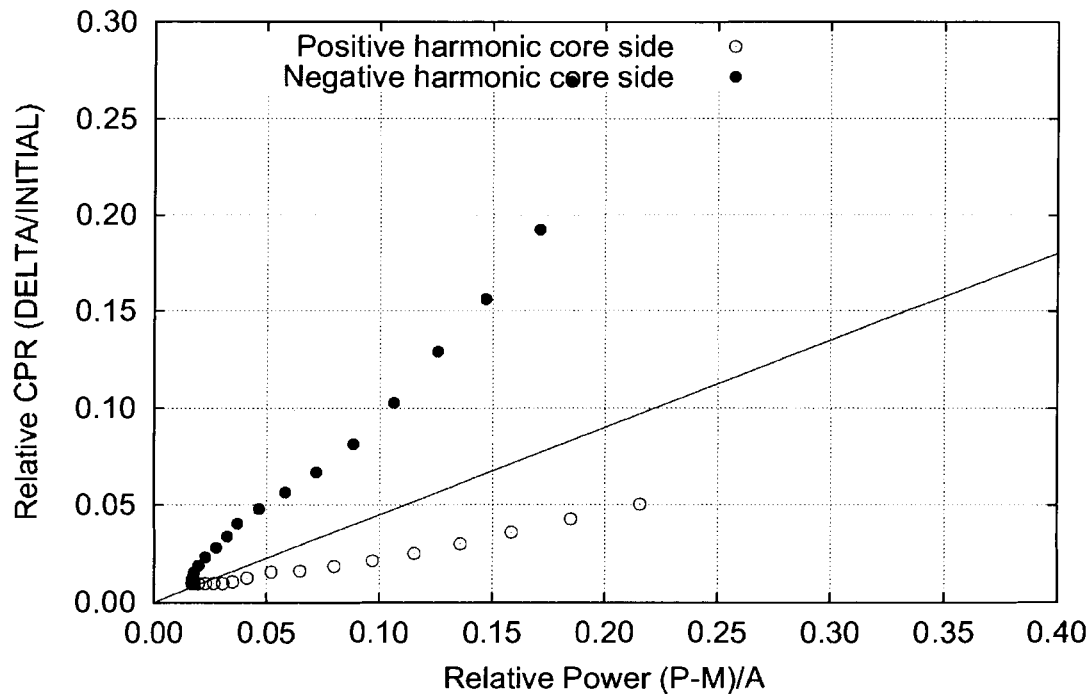


**Figure B-12 DIVOM Curve with Unstable Channel near the Neutral Line, 1.0% Regional, 2.0% Global Perturbation**

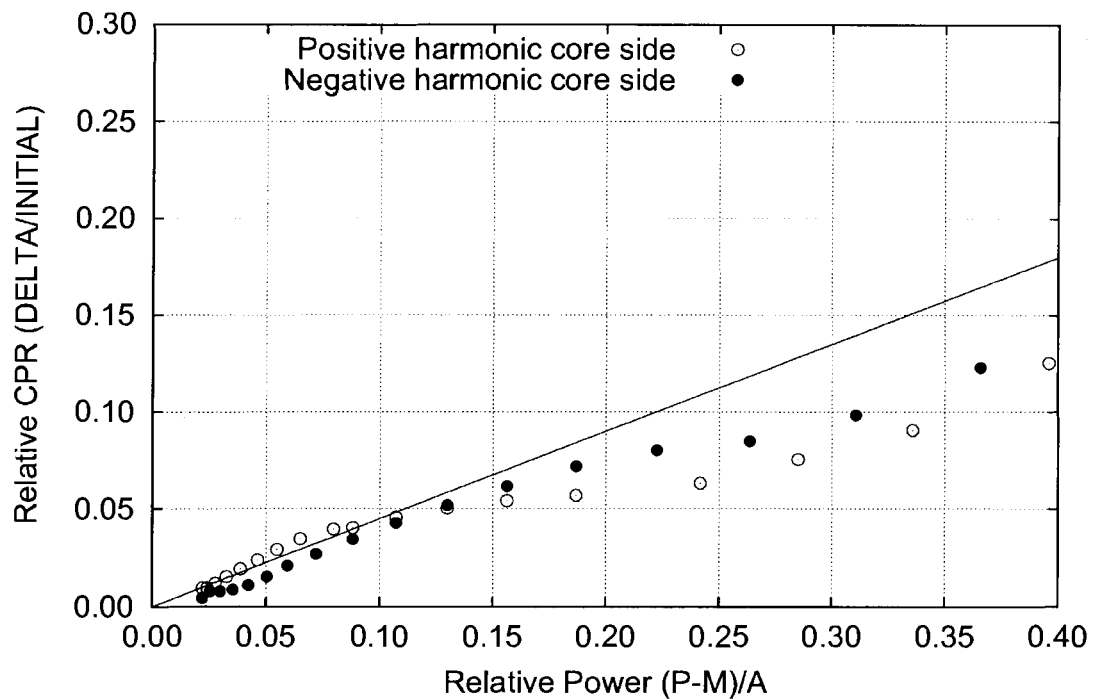


**Figure B-13 DIVOM Curve with Unstable Channel near the Neutral Line, 2.0% Regional, 1.0% Global Perturbation**

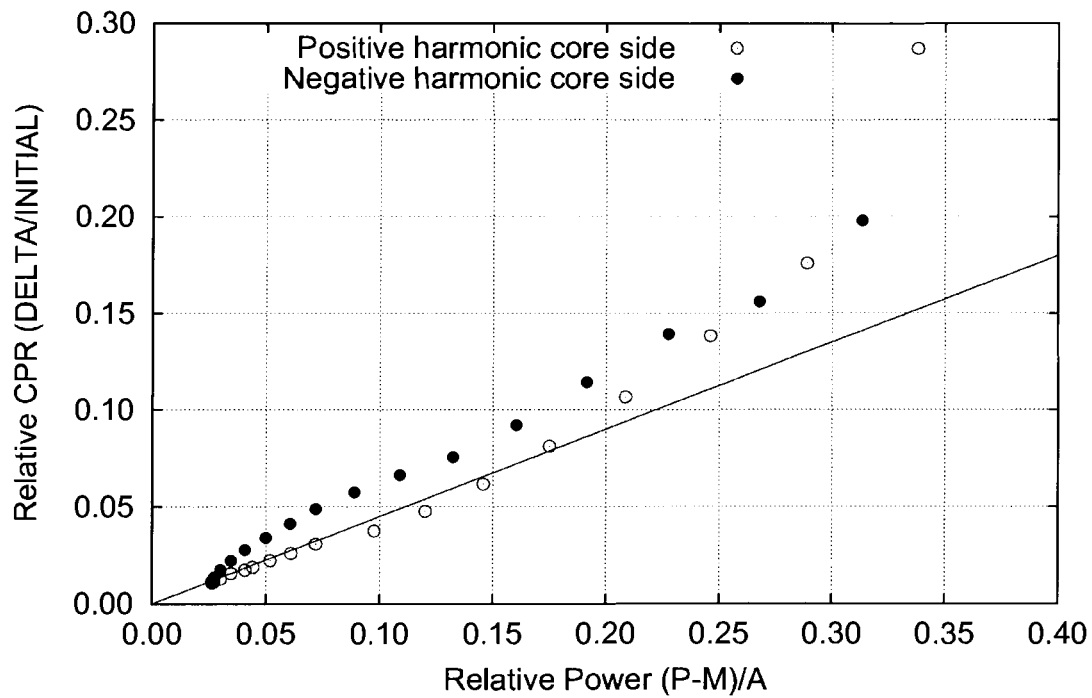


**Figure B-14 DIVOM Curve with Unstable Channel near the Neutral Line, 2.0% Regional, 2.0% Global Perturbation**

**Table B-1 DIVOM Slopes for Cases with the Hot Channel in the Harmonic Eye**

Perturbation %		Maximum DIVOM Slope	
Regional	Global	Positive Half	Negative Half
0.5	0.0	1.011	0.399
1.0	0.0	0.825	0.553
2.0	0.0	0.790	0.603
-0.5	0.0	0.669	0.655
-1.0	0.0	0.811	0.561
-2.0	0.0	0.868	0.631
2.0	-1.0	0.451	0.809
2.0	-2.0	0.531	1.007
2.0	1.0	0.768	0.439
2.0	2.0	1.059	0.435
1.0	-1.0	1.028	0.983
1.0	-2.0	1.026	1.367
1.0	1.0	1.019	0.287
1.0	2.0	1.129	0.564
Maximum		1.129	1.367

**Table B-2 DIVOM Slopes for Cases with the Hot Channel near the Neutral Line**

Perturbation %		Maximum DIVOM Slope	
Regional	Global	Positive Half	Negative Half
0.5	0.0	0.391	0.538
1.0	0.0	0.334	0.425
2.0	0.0	0.310	0.385
-0.5	0.0	0.533	0.397
-1.0	0.0	0.416	0.342
-2.0	0.0	0.386	0.309
2.0	-1.0	0.469	0.458
2.0	-2.0	0.844	0.651
2.0	1.0	0.427	0.400
2.0	2.0	0.849	0.632
1.0	-1.0	1.208	0.694
1.0	-2.0	1.399	0.228
1.0	1.0	0.798	0.670
1.0	2.0	0.235	1.458
Maximum		1.399	1.458



## Appendix C Relationship between Amplitude Setpoint and Period-Based Algorithm Confirmation Count

There are two theoretical models for calculating the number of confirmation counts,  $N_p$ , that are possible for an amplitude setpoint,  $S_p$ . The first model is the one described in Appendix E of Reference 2, which is rederived here. [

]

A derivation of the model described in Appendix E of Reference 2 is given below: The normalized oscillating signal is growing exponentially according to

$$s(t) = 1 + \varepsilon \cdot e^{\lambda_0 t} \cos\left(\frac{2\pi t}{\tau}\right) \quad (\text{C.1})$$

where the constant exponential growth parameter is related to the growth ratio and period according to

$$\lambda_0 = \frac{\log(G)}{\tau} \quad (\text{C.2})$$

and

- $\lambda_0$  Constant exponential growth parameter,
- $G$  Constant oscillation growth ratio,
- $\tau$  Constant oscillation period,
- $\varepsilon$  Minimum amplitude at the onset of oscillation, characteristic of the noise level,
- $t$  Time.

The noise level of  $\varepsilon = 0.015$  and  $G = 1.3$  are used for numerical demonstration in Appendix E of Reference 2.

The detection time,  $T$ , is defined as the time at which the signal amplitude reaches the setpoint,  $S_p$ . The magnitude term of the signal given by Equation C.1 can be substituted in Equation C.2 to get

$$S_p = 1 + \varepsilon \cdot e^{\log(G)T/\tau} \quad (C.3)$$

which is solved for  $T$  to get

$$T = \tau \frac{\log\left(\frac{S_p - 1}{\varepsilon}\right)}{\log(G)} \quad (C.4)$$

The number of counts per period is 2, which indicates that the PBDA accounts for the peaks and minima of each cycle. However, the first count is used to establish a base period and cannot be included in the confirmation count. Thus, the confirmation count is obtained from

$$N_p = \text{int}\left\{\frac{2T}{\tau} - 1\right\} \quad (C.5)$$

Eliminating  $T/\tau$  from Equations C.4 and C.5 gives

$$N_p = \text{int}\left\{\frac{2 \log\left(\frac{S_p - 1}{\varepsilon}\right)}{\log(G)} - 1\right\} \quad (C.6)$$

Equivalently, Equation C.5 can be substituted into Equation C.3 to get the amplitude peak as a function of the confirmation count.

$$S_p = 1 + \varepsilon \cdot e^{\frac{1}{2} \log(G)(1 + N_p)} \quad (C.7)$$

Numerical substitution in Equation C.7, with  $G = 1.3$  and  $\varepsilon = 0.015$ , reproduces Table E-1 of Reference 2.

[

]

[

]

[

]

## **Distribution**

### **Controlled Distribution**

#### Richland

J. S. Holm

A. W. Will

### **E-Mail Notification**

#### Richland

Y. M. Farawila

D. W. Pruitt

D. R. Tinkler

D. R. Todd

D. N. Ziabietsev

#### Erlangen

Stefan Opel

Franz Wehle

Florin Curca-Tivig